
Semi-Supervised Laplacian Learning on Stiefel Manifolds

Chester Holtz

Department of Computer Science
University of California San Diego
La Jolla, CA
chholtz@eng.ucsd.edu

Pengwen Chen

Department of Applied Mathematics
National Chung Hsing University
South District, Taichung, Taiwan

Alexander Cloninger

Department of Mathematics
University of California San Diego
La Jolla, CA

Chung-Kuan Cheng

Department of Computer Science
University of California San Diego
La Jolla, CA

Gal Mishne

Halicioğlu Data Science Institute
University of California San Diego
La Jolla, CA

Abstract

Motivated by the need to address the degeneracy of canonical Laplace learning algorithms in low label rates, we propose to reformulate graph-based semi-supervised learning as a nonconvex generalization of a *Trust-Region Subproblem* (TRS). This reformulation is motivated by the well-posedness of Laplacian eigenvectors in the limit of infinite unlabeled data. To solve this problem, we first show that a first-order condition implies the solution of a manifold alignment problem and that solutions to the classical *Orthogonal Procrustes* problem can be used to efficiently find good classifiers that are amenable to further refinement. Next, we address the criticality of selecting supervised samples at low-label rates. We characterize informative samples with a novel measure of centrality derived from the principal eigenvectors of a certain submatrix of the graph Laplacian. We demonstrate that our framework achieves lower classification error compared to recent state-of-the-art and classical semi-supervised learning methods at extremely low, medium, and high label rates. Our code is available on github¹.

1 Introduction

Semi-supervised learning is an important field in machine learning and statistics. Semi-supervised methods leverage both labeled and unlabeled data for tasks such as classification and regression. In semi-supervised learning (SSL), we are given a partially-labeled training set consisting of labeled examples and unlabeled examples. The goal is to leverage the unlabeled examples to learn a predictor that is superior to a predictor that is trained using the labeled examples alone. This setup is motivated by the high cost of obtaining annotated data in practical problems. Consequently, we are typically interested in the regime where the number of labeled examples is significantly smaller than the number of training points. For problems where very few labels are available, the geometry of the

¹anonymized for submission

unlabeled data can be used to significantly improve the performance of classic machine learning models. Additionally, the choice of labeled vertices is also a critical factor in this regime. In this work, we introduce a unified framework for graph-based semi-supervised and active learning at low label rates.

1.1 Graph-based semi-supervised Learning

A seminal work in graph-based semi-supervised learning is Laplace learning [56], which seeks a harmonic function that extends provided labels over the unlabeled vertices. Laplace learning, and its variants (notably, Poisson Learning [12]) have been widely applied in semi-supervised and graph-structured learning [53, 51, 5, 49].

In this work, we improve upon the state-of-the-art for graph-based semi-supervised learning at very low label rates. Classical Laplace learning and label propagation algorithms yield poor classification results [36, 4] in this regime. This is typically attributed to the fact that the solutions develop localized spikes near the labeled vertices and are nearly constant for vertices distant from labels. In other words, Laplace learning-based algorithms often fail to adequately propagate labels over the graph, given few labeled nodes. To address this issue, recent work has suggested imposing small adjustments to classical Laplace learning procedure. For example, p -Laplace learning [4, 41, 10, 11] for $p > 2$, and particularly for $p = \infty$, often yields superior empirical performance compared to Laplace learning at low label rates [16]. Other relevant methods for addressing low label rate problems include higher-order Laplacian regularization [54] and spectral classification [7, 55].

1.2 Active learning on graphs

The majority of existing active learning strategies typically involve evaluating the informativeness of unlabeled samples. For example, one of the most commonly used query frameworks is uncertainty sampling [38, 35, 33, 25] where the active learner queries the data samples which it is most uncertain about how to label. Most general uncertainty sampling strategies use some notion of margin as a measure of uncertainty [38, 35].

Many active learning algorithms that excel at low-label rates also employ strategies based on the connectivity of the graph, e.g. the degree centrality or cut structure [13, 19, 31]. Related work includes geometric landmarking methods, which seek to maximize coverage of the collected samples. For example, [40, 24] propose geodesic distance-based strategies to greedily add new landmarks with large cumulative geodesic distance to existing landmarks. However, these methods are computationally prohibitive on most benchmarks. Particularly relevant to our work are algebraic landmarking methods. In particular, [48] proposed an algebraic reconstruction error bound based on the Gershgorin circle theorem (GCT) [17] and an associated greedy algorithm based on this bound. However, this method suffers from high complexity due to logarithmic computations of a large matrix.

1.3 Contribution

In this work, we propose to solve a natural semi-supervised extension of Laplacian Eigenmaps and spectral cuts, which are well-posed in the limit of unlabeled data. Our extension is initially motivated by the optimization-based perspective of Laplacian Eigenmaps as a Rayleigh Quotient minimization problem over all labeled and unlabeled vertices. We show that a natural partitioning of the problem yields a more general quadratically constrained quadratic program over the unlabeled vertices. We then generalize the sequential subspace (SSM) framework originally proposed to solve similar problems in \mathbb{R}^n to $\mathbb{R}^{n \times k}$ and we develop an associated active learning scheme.

To summarize, our contributions are:

1. We introduce a natural formulation of graph semi-supervised learning as a rescaled quadratic program on a compact Stiefel Manifold, i.e. a generalization of a *Trust-Region Subproblem*.
2. We describe a scalable approximate method, globally convergent iterative methods, and a graph cut-based refinement scheme and demonstrate robustness in a variety of label rate regimes.
3. We introduce a score to characterize informative samples based on the principal eigenvectors of the *grounded Laplacian*.

4. We compare our approach to competing semi-supervised graph learning algorithms and demonstrate state-of-the-art performance in low, medium, and high label rate settings on MNIST, Fashion-MNIST, and CIFAR-10.

The rest of the paper is organized as follows. In Section 2 we briefly introduce Laplacian Eigenmaps and our supervised variant, and then provide a detailed motivation for the algorithm. Our formulation is presented in Section 3. Approximate and iterative algorithms are presented in Section 3.1 and our approach to active learning at low label rates is presented in Section 4. In Section 5 we present numerical experiments. We conclude and discuss future work in Section 6.

2 Preliminaries and Related Work

We assume the data can be viewed as lying on a graph, such that each vertex is a data-point. Let $\mathcal{V} = \{v_1, v_2, \dots, v_M\}$ denote the M vertices of the graph with edge weights $w_{ij} \geq 0$ between v_i and v_j . We assume that the graph is symmetric, so $w_{ij} = w_{ji}$. We define the degree $d_i = \sum_{j=1}^n w_{ij}$. For a multi-class classification problem with k classes, we let the standard basis vector $e_i \in \mathbb{R}^k$ represent the i -th class (i.e. a ‘‘one hot encoding’’). Without loss of generality, we assume the first m vertices $l = \{v_1, v_2, \dots, v_m\}$ are given labels $y_1, y_2, \dots, y_m \in \{e_1, e_2, \dots, e_k\}$, where $m \ll M$. Let n denote the number of unlabeled vertices, i.e. $n = M - m$. The problem of graph-based semi-supervised learning is to smoothly propagate the labels over the unlabeled vertices $\mathcal{U} = \{v_{m+1}, v_{m+2}, \dots, v_M\}$. The compact *Stiefel Manifold* is denoted

$$\text{St}(n, k) = \{X \in \mathbb{R}^{n \times k} : X^\top X = I\}. \quad (1)$$

Note that the projection of a matrix $X \in \mathbb{R}^{n \times k}$ onto $\text{St}(n, k)$, denoted $[X]_+ := \arg \min\{\|X_s - X\|_F : X_s \in \text{St}(n, k)\}$ is given by

$$[X]_+ = UV^\top, \quad (2)$$

where $X = U\Sigma V^\top$ is the singular value decomposition. Given a graph and a set of labeled vertices, the Laplace learning algorithm [56] extends the labels over the graph by solving the following problem

$$\left. \begin{aligned} x(v_i) &= y_i, & \text{if } 1 \leq i \leq m \\ \mathcal{L}x(v_i) &= 0, & \text{if } m+1 \leq i \leq M \end{aligned} \right\} \quad (3)$$

where \mathcal{L} is the unnormalized graph Laplacian given by $\mathcal{L} = D - W$, D is a diagonal matrix whose elements are the node degrees, and $x : \mathcal{V} \rightarrow \mathbb{R}^k$. The prediction for vertex v_i is determined by the largest component of $x(v_i)$:

$$\arg \max_{j \in \{1, \dots, k\}} \{x_j(v_i)\}. \quad (4)$$

Note that Laplace learning is also called *label propagation (LP)* [57], since the Laplace equation eq. (16), can be solved by repeatedly replacing $x(v_i)$ with the weighted average of its neighbors.

The solution of Laplace learning eq. (16), is the minimizer of the following gradient regularized variational problem with label constraints $x(v_i) = y_i$:

$$\min_{x \in \ell^2(\mathcal{V})} \left\{ \|\nabla x\|_{\ell^2(\mathcal{V}^2)}^2 \mid x(v_i) = y_i, 1 \leq i \leq m \right\} \quad (5)$$

3 Spectral Embeddings with Supervision

In Laplacian Eigenmaps [8], one seeks an embedding of the vertices via the eigenfunctions of the Laplacian corresponding to the smallest nontrivial eigenvalues. Equivalently, this can be expressed as the following *Quadratically Constrained Quadratic Program (QCQP)* over the vertices of the graph:

$$\min_{X_0} \langle X_0, \mathcal{L}X_0 \rangle \quad \text{s.t. } X_0^\top X_0 = I, \quad \mathbf{1}^\top X_0 = 0 \quad (6)$$

where $\langle A, B \rangle$ is the trace of the matrix $A^\top B$ and $\mathbf{1}$ is the all-ones vector. The notation $X_0 \in \mathbb{R}^{M \times k}$ is the mapping of the M vertices to a k -dimensional space. In the case where $k = 1$, eq. (6) is also known in the numerical analysis literature as a *Rayleigh quotient minimization problem* [18]. Despite its nonconvexity, a unique (up to orthogonal transformations) global solution is given by the set of eigenvectors of \mathcal{L} corresponding to the smallest k nontrivial (nonzero) eigenvalues of \mathcal{L} .

We first extend this framework with supervision, similarly to Laplace learning in eq. (5). Additionally, to facilitate the supervised decomposition, we rescale I uniformly by $p = M/k$, the balanced proportion of samples associated with each class:

$$\min_{X_0} \langle X_0, \mathcal{L}X_0 \rangle \quad \text{s.t. } X_0^\top X_0 = pI, \mathbf{1}^\top X_0 = 0, (X_0)_i = y_i, i \in [m] \quad (7)$$

The associated prediction is then $\ell(x_i) = \arg \max_{j \in \{1, \dots, k\}} (X_0)_{ij}$. Next, we show how supervision naturally leads to a partitioning of the problem. We denote the submatrices of X_0 and \mathcal{L} corresponding to the n unlabeled vertices $\mathcal{U} \subseteq \mathcal{V}$ and m labeled vertices $\mathcal{l} \subseteq \mathcal{V}$ as $X_{\mathcal{U}}, X_{\mathcal{l}}$ and $L_{\mathcal{U}}, L_{\mathcal{l}}$, respectively. More concretely, $\mathcal{L} = \begin{bmatrix} L_{\mathcal{l}} & L_{\mathcal{U}\mathcal{l}} \\ L_{\mathcal{l}\mathcal{U}} & L_{\mathcal{U}} \end{bmatrix}$ and $X_0 = \begin{bmatrix} X_{\mathcal{l}} \\ X_{\mathcal{U}} \end{bmatrix}$. Then, in conjunction with considering $X_{\mathcal{l}}$ fixed, the problem in eq. (7) may be expressed as

$$\min_{X_{\mathcal{U}}} \langle X_{\mathcal{U}}, L_{\mathcal{U}}X_{\mathcal{U}} \rangle - \langle X_{\mathcal{U}}, B_0 \rangle \quad \text{s.t. } X_{\mathcal{U}}^\top X_{\mathcal{U}} = C_{\mathcal{U}}, \mathbf{1}^\top X_{\mathcal{U}} = -r^\top \quad (8)$$

where $B_0 = 2 \cdot L_{\mathcal{U}\mathcal{l}}X_{\mathcal{l}}, C_{\mathcal{U}} = pI - X_{\mathcal{l}}^\top X_{\mathcal{l}} = (p - \tilde{p})I$, where $\tilde{p} = m/k$, and $r = (\mathbf{1}^\top X_{\mathcal{l}})^\top = \tilde{p}\mathbf{1}^\top \in \mathbb{R}^k$ are fixed parameters, and $X_{\mathcal{U}}$ are the decision variables. It should also be mentioned that $L_{\mathcal{U}}$ is known in the literature as a *grounded Laplacian*.

In general, the quadratic equality constraint poses a significant challenge from an optimization standpoint. We propose to address this problem directly by solving an equivalent rescaled problem. By introducing terms to eliminate the linear constraint, we show how the problem may be rescaled and efficiently and robustly solved as a quadratic program on a compact *Stiefel Manifold*. The associated solution to this problem can then be used to determine the labels of the unlabeled vertices, as in Laplace learning (eq. (4)).

To eliminate the linear constraint, we introduce two adjustments: first, let $(X)_i = (X_{\mathcal{U}})_i + \frac{1}{n}r^\top$ denote a row-wise centering transformation with respect to the labeled nodes. This yields the new constraint $\mathbf{1}^\top X = 0$ and yields $C = C_{\mathcal{U}} - \frac{1}{n}rr^\top$ for X . Second, we introduce the projection $P = I - \frac{1}{n}\mathbf{1}\mathbf{1}^\top$ onto the subspace orthogonal to the vector $\mathbf{1} \in \mathbb{R}^n$, i.e., $\mathbf{1}^\top(PX) = 0$, which projects vectors onto the set of mean-zero vectors. To obtain a solution limited to this subspace, we introduce the substitutions $B = P(B_0 - L_{\mathcal{U}}\frac{1}{n}\mathbf{1}r^\top)$ and $L = PL_{\mathcal{U}}P$ which implies $\mathbf{1}^\top B = 0$. Consider the substitution $X \leftarrow XC^{1/2}$. The equivalent, rescaled problem is then

$$\min_{X: X \in \text{St}(n, k)} \langle X, LXC \rangle - \langle X, BC^{1/2} \rangle. \quad (9)$$

Note that this problem is a generalization of well-known problems that arise in trust-region methods, optimization of a nonconvex quadratic over a unit ball or sphere [42, 15], i.e. problems of the form

$$\min_{x \in \mathbb{R}^n: \|x\|=1} \langle x, Lx \rangle - \langle x, b \rangle.$$

We define the Lagrangian of eq. (9) where $\Lambda \in \mathbb{R}^{k \times k}$ are the Lagrange multipliers:

$$\langle X, LXC \rangle - \langle X, BC^{1/2} \rangle - \langle \Lambda, (X^\top X - I) \rangle. \quad (10)$$

The first-order condition is then

$$LXC = BC^{1/2} + X\Lambda \quad (11)$$

for some Λ . Solutions X that satisfy eq. (11) are *critical points* or *stationary points*. In general, there could exist many critical points that satisfy this condition. In the appendix we show that at these ‘‘stationary points’’ (maximizers, minimizers, or saddle points), (1.) the eigenvalues of Λ characterize the optimality of X and (2.) finding good critical points necessitates computation of L ’s eigenvectors.

3.1 Semi-supervised spectral learning algorithms

In this section, we introduce approximate and iterative methods to solve eq. (9). In theory, as we show in the appendix, one can start with an arbitrary initialization to obtain a critical point of eq. (9) using a variety of projection- or retraction-based gradient methods, with the descent direction given by the gradient of eq. (9) and projection given by eq. (2). However, the empirical rate of convergence depends significantly on the initialization of the embedding matrix X . In order to improve convergence of our method, we first introduce and motivate an efficient method based on Procrustes Analysis [46] to approximately compute critical points of the *unscaled* objective ($C = I$). This approximation is appropriate in the limit of few labeled examples or unlimited unlabeled data: since $C = (p - \tilde{p})I - \frac{\tilde{p}^2}{n}\mathbf{1}\mathbf{1}^\top$, then $C \rightarrow pI$ in the limit of $\frac{m}{n} \rightarrow 0$.

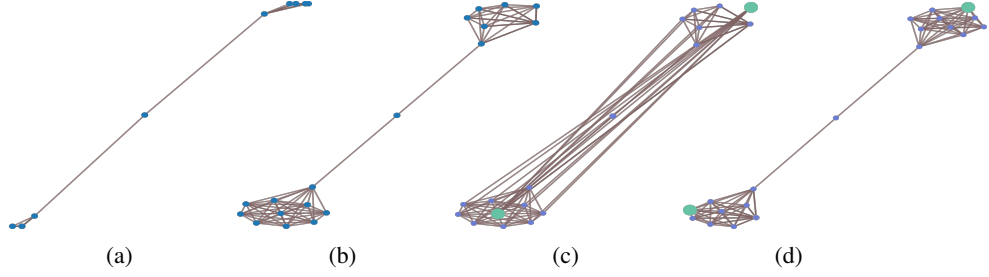


Figure 1: **Eigenvector method and projection example on the barbell graph.** (a): Embedding into \mathbb{R}^k via Laplacian Eigenmaps. (b): Several iterations of gradient-based repulsion are applied to remove vertex overlaps for better visualization. (c): Consider taking an arbitrary vertex from each clique and assigning it a label (green vertices). Spectral embeddings are likely *inconsistent* with labeled vertices. (d): Procrustes embedding. The orthogonal transform Q is derived from Prop. 3.1 and applied to X ; XQ resolves the discrepancy between the embeddings and the labeled vertices.

3.2 Efficient approximation via Orthogonal Procrustes

Here we propose an efficient way to compute approximate critical points of eq. (9). First we solve the canonical eigenvalue problem $\min_X \text{tr}(X^\top LX)$ subject to a constraint on the second moment of X : $X^\top X = I$, yields X are the eigenvectors of L . Second, we appropriately transform the solution so that $X^\top B$ is positive definite (i.e. satisfies a necessary condition for first-order optimality).

Proposition 3.1 (Definiteness conditions of $X^\top B$). *Assume $C = I$. Note the first term of the objective in eq. (9) satisfies the invariance $\langle X, LX \rangle = \langle \tilde{X}, L\tilde{X} \rangle$, where $\tilde{X} = XQ$ for any orthogonal $Q \in \mathbb{R}^{k \times k}$. Suppose X is a local minimizer of eq. (9). Then, $X^\top B \succcurlyeq 0$ and symmetric.*

A consequence of this is the following: Let the SVD of $X^\top B = U_B D_B V_B^\top$ and let $Q = U_B V_B^\top$. Algorithmically, this implies that projecting X onto Q decreases the objective of eq. (9) (assuming $C = I$). Note, in practice, we can additionally rescale predictions by taking $X \leftarrow XC^{1/2}$ to properly observe the constraint on the second moment of X .

This step can be interpreted as an alignment step, where we find an orthogonal transformation Q that aligns unlabeled vertices with their neighboring labeled vertices, and apply this transformation to all unlabeled vertices. We briefly describe the connection with Orthogonal Procrustes Analysis [46]. Let X be feasible, i.e. $X^\top X = I$. Note that the invariance is nothing but $\text{tr}(X^\top LX) = \langle X, LX \rangle = \langle XQ, LXQ \rangle$ for any orthogonal Q . Thus,

$$\arg \min_{Q: Q \in \text{St}(k, k)} \langle XQ, LXQ \rangle - \langle XQ, B \rangle = \arg \max_{Q: Q \in \text{St}(k, k)} \langle XQ, B \rangle = \arg \min_{Q: Q \in \text{St}(k, k)} \|XQ - B\|_F^2. \quad (12)$$

This problem is the canonical Orthogonal Procrustes problem in $\mathbb{R}^{k \times k}$ in the context of finding an alignment between the axis-aligned labeled vertices and their neighborhood of unlabeled vertices. We demonstrate the effect of this procedure in Figure 1. In Figure 1a–b, we plot the first pair of eigenvectors corresponding to the smallest two nonzero eigenvalues associated with a barbell graph. In Figure 1c, we pick a random pair of vertices v_i and v_j with coordinates x_i and x_j from each clique and assign labels $y_i = x_i$ and $y_j = x_j$. Under this labeling, we say that the embedding is *inconsistent*. In other words, a linear predictor in the space spanned by the embedding would be incapable of recovering a separating hyperplane that accurately classifies the unlabeled samples. We then show that by applying the approximate method based on Procrustes Analysis introduced in Section 3.2, we recover an embedding which is *consistent* with the labels.

Alternatively, the projection and Q -transform can be interpreted as performing orthogonal multivariate regression in the space spanned by the first k nontrivial eigenvectors of L :

$$Q = \arg \min_{Q: Q \in \text{St}(k, k)} \sum_{i \in [m]} \|x_i Q - y_i\|_2^2,$$

where $Q \in \mathbb{R}^{k \times k}$ and predictions are given by XQ . Note that this is similar in principal to the Semi-Supervised Laplacian Eigenmaps (SSL) algorithm [7], which solves an ordinary least squares problem using eigenvectors X of the Laplacian as features:

$$Q = \arg \min_Q \sum_{i \in [m]} \|x_i Q - y_i\|_2^2.$$

Crucially, the orthogonality constraint on Q ensures that the solution remains feasible, i.e. that $XQ \in \text{St}(n, k)$. Furthermore, we show in our experiments that this feasibility significantly improves generalization at very low label rates in comparison to standard Laplacian Eigenmaps SSL. These interpretations serve to motivate our initialization and subsequent refinement. In particular, Zhou and Srebro [55] consider the limiting behavior of Laplacian Eigenmaps SSL and show that it is non-degenerate in the limit of infinite unlabeled data.

3.3 Iterative refinement with SSM and KL

To refine solutions produced by the Procrustes algorithm into solutions to eq. (9), we introduce an efficient iterative method capable of global convergence to high-quality stationary points. Motivated by the similarity between eq. (9) and standard trust-region subproblems, we develop the framework of the *Sequential Subspace Method (SSM)*. In the $k = 1$ and $C = I$ case, SSM has been applied to Trust-Region sub-problems with remarkable empirical results [21] and robust global convergence guarantees [20], even for so-called degenerate problems. SSM-based algorithms generate a sequence of iterates X_t by solving a series of rescaled quadratic programs (of the same form as eq. (9)) in subspaces of dimension much smaller than that of the original problem (where $d = |V|$, the number of vertices in the graph).

Although stationary points can be recovered via generic iterative project-descent procedures—gradient-based or Newton-based descent directions (e.g. via SQP or trust-region-type algorithms), SSM is a computationally friendly algorithm designed to address scalability with respect to large problems. We develop a SSM on the Stiefel manifold, which is inspired by the 1-dimensional algorithm of [21], originally proposed to solve large trust-region subproblems.

At step t a tiny subspace, S_t , of dimension $4k$ is derived from the current iterate X_t , the gradient of the objective of eq. (9) $g_t = LX_t C - BC^{1/2}$, an SQP (i.e. Newton’s method applied to the first-order optimality system X_t) iterate X_{sqp} derived in Prop. 3.2, and the principal eigenvectors of L . The Sequential Quadratic Programming (SQP) framework [37] is adapted to compute X_{sqp} . X_{t+1} is then generated by solving eq. (9) in this small subspace. Crucially, we highlight that when the eigenvectors of L are included in the subspace, the sequence of iterates generated by SSM exhibits the following global convergence property, which we discuss further in the appendix.

Theorem 1 (Global convergence of SSM). *A limit X_* of $\{X_1, X_2, \dots, X_t, \dots\}$ generated by SSM is a local minimizer of eq. (8).*

To further adjust predictions, we introduce a multi-class Kernighan-Lin (KL) refinement algorithm to iteratively adjust the classification to improve a cut-based cost. Critically, this method is efficient (linear-time) and, in contrast to the gradient-based refinement method proposed in PoissonMBO [12], robust to the nonconvexity of the cut objective.

3.4 Sequential Subspace Method (SSM) Algorithm

Here we introduce an efficient iterative method capable of global convergence to high-quality stationary points. We apply this method to refine the approximate solutions produced using the method introduced in Section 3.2. Motivated by the similarity between eq. (9) and standard trust-region subproblems, we apply the framework of SSM. In the $k = 1$ and $C = I$ case, SSM has been applied to Trust-Region sub-problems with remarkable empirical results [21] and robust global convergence guarantees [20], even for so-called degenerate problems. At a high level, SSM-based algorithms generate a sequence of iterates X_t by solving a series of rescaled quadratic programs (of the same form as eq. (9)) in subspaces of dimension much smaller than that of the original problem.

At step t , we introduce a subspace S_t derived from the current iterate X_t , the gradient of the objective of Prob. eq. (9) $g_t = LX_t C - BC^{1/2}$, an SQP (i.e. Newton’s method applied to the first-order optimality system X_t) iterate X_{sqp} derived in Prop. 3.2, and the principal eigenvectors of L . The Sequential Quadratic Programming (SQP) framework [37] is applied to compute X_{sqp} .

Following the principle of SQP, we introduce the SQP direction Z according to the linearization of eq. (11), the first-order conditions of eq. (9):

$$(LZC - ZA) - X\Delta = E := BC^{1/2} - (LXC - X\Lambda), \quad X^\top Z = 0$$

Proposition 3.2 (SQP iterate of the Lagrangian of eq. (10)). *Assume Λ is symmetric. Let $P^\perp = I - X^\top X$ be the projection onto the orthogonal complement of the column space of X and $\Lambda C^{-1} = U \text{diag}([\lambda_1, \dots, \lambda_k]) U^{-1}$ be the eigenvector decomposition of ΛC^{-1} . The Newton direction Z of X via the linearization of the first-order conditions is*

$$Z = OU^\top, \quad (13)$$

where each column of O , $o_j = (P^\perp L P^\perp - \lambda_j P^\perp)^\dagger B C^{-1} u_j$.

Algorithm 1 SQP Update

Input: Partial Laplacian L , affine term B , intermediate feasible iterate X_t , scaling term C

Output: j - th columns of Newton updates— Δ_j, Z_j

```

1: function SQP( $L, \Lambda_t, B, X_t$ )
2:    $\Lambda_t = X_t^\top (L X_t C - B C^{1/2})$ 
3:    $U \text{diag}([\lambda_1, \dots, \lambda_k]) U = \Lambda C^{-1} = C^{-1/2} \Lambda_t C^{-1/2}$ 
4:   init  $O, P^\perp = I - X^\top X$ 
5:   for  $j \in [k]$  do
6:      $o_j = (P^\perp L P^\perp)^\dagger B C^{-1} u_j$ 
7:   end for
8:   return  $OU^\top$ 
9: end function

```

Alg. 1 presents the detailed steps involved in the computation of the Newton directions, i.e. Prop. 3.2. In Section 3.4, we discuss its computational cost.

Although stationary points can be recovered via an iterative project-descent procedure using gradient-based or SQP-based descent directions, we introduce the Sequential Subspace Method (SSM) in Alg. 2: a computationally friendly algorithm to address scalability with respect to large problems. Our development of SSM is inspired by the 1-dimensional algorithm of [21], originally proposed to solve large trust-region subproblems. In other words, instead of solving eq. (8) directly as previously mentioned, we instead solve a sequence of quadratic programs in subspaces of much smaller dimension relative to the size of the graph (the dimensions of L). SSM generically involves repeating the following pair of steps:

1. Compute the SQP direction $Z = \text{SQP}(L, \Lambda, B, X)$ as defined in Prop. 13 and Alg.1, line 5. Let V be the orthogonal matrix consisting of columns in S (Alg.2, lines 6 and 7), where

$$S = \text{span}(X_t, Z_t, u, g_t).$$

2. SSM generates an approximation of (X, Λ) and an approximation of the smallest pair of eigenvalues σ and eigenvectors u of L in the subspace S ,

$$[X, \Lambda, u, \sigma] = \text{SSM}(L, B, S)$$

consider the approximation $X = V\tilde{X}$ for some \tilde{X} . Compute

$$\min_{\tilde{X} \in \text{St}(\tilde{n}, k)} F_S := \min_{\tilde{X}} F(\tilde{X}; V^\top L V, V^\top B). \quad (14)$$

Note that eq. (14) is solved using the Projected Gradient Method, where the projection is given by eq. (2): $[X]_+ = UV^\top$. We update Λ according to the least-squares estimate derived from the first order condition in eq. (11) $\Lambda = X^\top (A X C - B C^{1/2})$.

We highlight that the sequence of iterates generated by SSM exhibits the following global convergence property, which we discuss further in the appendix.

Theorem 1 (Global convergence of SSM). *A limit X_* of $\{X_1, X_2, \dots, X_t, \dots\}$ generated by SSM is a local minimizer of eq. (8).*

Algorithm 2 Sequential Subspace Minimization

Input: Partial Laplacian matrix L , unit vector u **Output:** Embedding coordinates X

```
1: function SSM( $A, u$ )
2:    $L \leftarrow D - A$  ▷ Compute the graph Laplacian
3:   Initialize  $X$  according to Sec 3.2.
4:   while not converged do
5:      $Z \leftarrow SQP(L, \Lambda, B, X, u)$  ▷ Eq. 13 & Alg. 2
6:      $S \leftarrow \text{span}(X_t, Z_t, u, g_t)$ 
7:      $V \leftarrow QR(\text{col}(S))$ 
8:      $\tilde{L} \leftarrow V^\top LV, \tilde{B} \leftarrow V^\top B$ 
9:      $\tilde{X} \leftarrow \min_{X; X^\top X = I} F(X; \tilde{L}, \tilde{B})$  ▷ Solve Eq. 9 in  $S$ 
10:     $X_t \leftarrow V^\top \tilde{X}$  ▷ Lifted coordinates
11:     $t \leftarrow t + 1$ 
12:  end while
13:  return  $X_t$ 
14: end function
```

3.5 Complexity of SSM

In this section, we discuss the computational cost of our method, dominated by the SQP routine to compute the SQP directions. We claim that the per-iteration complexity of our algorithm is T_{matrix} , where T_{matrix} is the complexity of each call to a sparse matrix (i.e. Laplacian, more generally an M -matrix) solver. In particular, the QR-decomposition of $\text{col}(S)$ takes time linear in n . Likewise, fast, nearly linear-time solvers exist for solving Laplacian and Laplacian-like systems that are robust to ill-conditioning [43]. We adopt Multigrid preconditioned conjugate gradient due to its empirical performance. We further note that the SSM procedure itself exhibits quadratic rates of convergence for nondegenerate problems and global convergence with *at least* linear rates, even when the problem exhibits certain degenerate characteristics [20].

3.5.1 Computation of the descent direction Z

In Sec 3.3, we express the SQP direction Z as the solution to the system characterized by the linearization of the first order optimality conditions. Namely, within each iteration of our procedure, we compute the Lagrangian multipliers as well as the SQP update for X as defined in eq. (13). As in Newton’s method for unconstrained problems, SQP-based methods necessitate computation of inverse-vector products involving symmetric PSD matrices.

We assume that by exploiting the sparsity of L , vector-vector and matrix-matrix multiplication can be done in linear time. In Alg. 1, we present the the SQP routine. The computation in line 3 involves an eigenvalue decomposition of a small $k \times k$ matrix. Thus, the primary overhead of our method lies in the computation of each column of O ; $o_j, j = 1, \dots, k$, which necessitates computation of k Laplacian-like pseudoinverse-vector products.

3.6 Cut-based refinement

In this section, we provide a detailed overview of the Kernighan-Lin (KL) algorithm and our multi-class extension.

The Kernighan-Lin algorithm [27] iteratively improves a given a disjoint bipartition of \mathcal{V} : $(\mathcal{V}_1, \mathcal{V}_2)$ such that $\mathcal{V}_1 \cup \mathcal{V}_2 = \mathcal{V}$, by finding subsets of each partition $A \subset \mathcal{V}_1, B \subset \mathcal{V}_2$ and then moving the nodes in A and B to the opposite block. More concretely, the Kernighan-Lin algorithm repeatedly finds candidate sets A, B to be exchanged until it reaches a local optimum with respect to the cut objective. Notably, the algorithm has the desirable tendency to escape poor local minima to a certain extent due to the way in which the sets A and B are created. This is one of the key features of the algorithm, and is a critical advantage over gradient-based methods for partitioning refinement, such as the MBO method presented in [12].

Algorithm 3 Kernighan-Lin refinement

Input: KNN weights W **Output:** Predictions X

```
1: Compute  $g(v)$  for all  $v \in \mathcal{V}$ 
2: while not converged do
3:   for each pair of  $\binom{n}{2}$  partitions (classes)  $\mathcal{V} = (\mathcal{V}_1, \mathcal{V}_2)$  do
4:     ordered list  $l \leftarrow \emptyset$ 
5:     unmark all vertices  $v \in V$ 
6:     for  $i = 1$  to  $n = \min(|\mathcal{V}_1|, |\mathcal{V}_2|)$  do
7:        $(v_1, v_2) \leftarrow \arg \max_{v_1, v_2} g(v_1, v_2)$ 
8:       update  $g$ -values for all  $v \in N(v_1) \cup N(v_2)$ 
9:       add  $(v_1, v_2)$  to  $l$  and mark  $v_1, v_2$ 
10:    end for
11:     $k^* \leftarrow \arg \max_k \sum_{i=1}^k g(v_i, w_i)$ 
12:    Update  $(\mathcal{V}_1, \mathcal{V}_2)$ : swap  $(v_i, w_i) \in l, i = 1, \dots, k^*$ 
13:  end for
14: end while
```

The gain of a vertex v is defined $g(v) = \sum_{j|\ell(v_i)=\ell(v_j)} W_{ij} - \sum_{j|\ell(v_i) \neq \ell(v_j)} W_{ij}$, i.e. the reduction in the cut cost when the vertex v is moved from partition V_1 to partition V_2 . Thus, when $g(v) > 0$ we can decrease the cut by $g(v)$ by moving v to the opposite block. Let $g(v, w)$ denote the gain of exchanging v and w between V_1 and V_2 . Analogously, if v and w are not adjacent, then the gain is $g(v, w) = g(v) + g(w)$. If v and w are adjacent, then $g(v, w) = g(v) + g(w) - 2\omega(v, w)$.

The KL algorithm characterizes each vertex in G as having one of two states: marked or unmarked. At each pass of the algorithm, each node is unmarked. A KL pass proceeds by iteratively finding an unmarked pair $v \in \mathcal{V}_1$ and $w \in \mathcal{V}_2$ for which $g(v, w)$ is maximum (note that $g(v, w)$ is not necessarily positive), marking v and w , and updating the gain values of each of remaining unmarked nodes (i.e. the neighbors of v and w) assuming an exchange between v and w . This procedure repeats $p = \min(|\mathcal{V}_1|, |\mathcal{V}_2|)$ times.

After p iterations, we have an ordered list l of vertex pairs $(v_i, w_i), i = 1, \dots, p$. The swap-sets A and B are derived by finding the smallest index $k \in \{0, \dots, p\}$ such that $P = \sum_{i=1}^k g(v_i, w_i)$ is maximum. Then, $A := \bigcup_{i=1}^k \{v_i\}$ and $B := \bigcup_{i=1}^k \{w_i\}$. A nonzero k implies a reduction of the cut cost if A and B are exchanged. In this case, the exchange is performed and a new pass is instantiated. Otherwise, the KL iterations conclude.

Note that KL is typically performed over bi-partitions. We extend this framework to k -partitions in Algorithm 3 by considering a randomly ordered set of $\binom{k}{2}$ pairs of classes (as defined by the predictions made on the vertex set) and performing KL on the subgraph restricted to these vertices. This procedure continues iteratively until all $\binom{k}{2}$ pairs have been exhausted. Then, if convergence or a predetermined number of iterations has not been reached, a new random sequence is generated and the procedure continues.

4 Graph-Based Active Learning

In this section, we introduce an active-learning scheme motivated by the criticality of label selection at low label rates and the benefits of diversity sampling. In the low label-rate regime, it is well-known that active learning strategies which emphasize *exploration* of the sample-space, i.e. *diversity* of the labeled samples, outperform those that rely on *exploitation* of a classifiers decision boundary, e.g. notions of margin [34]. Therefore, we propose a computationally efficient technique inspired by algebraic methods for selecting landmarks in graphs—i.e. a method that aims to select well-connected vertices diversely over the graph (vertices with large degree that are maximally separated) according to the spectral properties of the Laplacian.

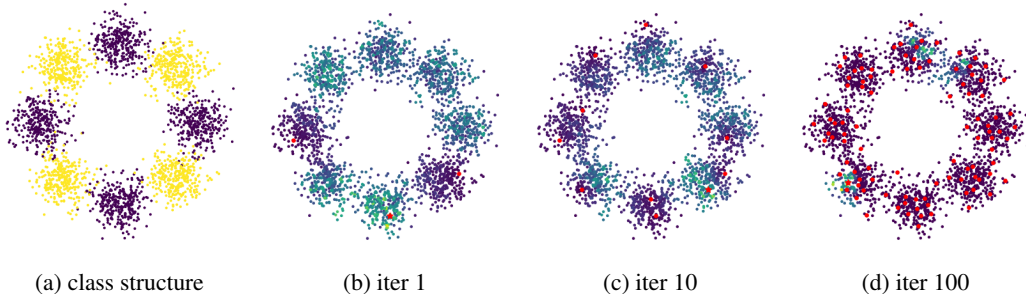


Figure 2: **Visualization of the lower-bound estimate on a ring of Gaussians** Labeled points are annotated as red circles. Points to be labeled are marked as red stars. Brighter regions of the heatmap indicate vertices with higher score.

4.1 Spectral score for diversity sampling on graphs

We propose to select vertices from the set of unlabeled vertices according to the following measure:

$$\arg \max_{v_i} \{s(v_i) := \tilde{d}_i u_i^2\} \quad (15)$$

where \tilde{d}_i denotes the degree of vertex i defined on the sub-graph associated with the set of unlabeled vertices, \mathcal{U} and u_i corresponds to the i -th entry of u , the solution to the boundary-constrained eigenvalue problem:

$$\left. \begin{aligned} \mathcal{L}u_i &= \lambda u_i, & \text{if } m+1 \leq i \leq M \\ u_i &= 0, & \text{if } 1 \leq i \leq m \end{aligned} \right\}. \quad (16)$$

Note that $\text{supp}(u)$ is nothing but the entries of the eigenvector corresponding to the smallest eigenvalue of $L_{\mathcal{U}}$. Naturally, u_i encodes various notions of centrality. Notably, Cheng et al. [14] demonstrate an intimate connection between the solution u in eq. (16) for a normalized random walk Laplacian and the absorption time of a random walk / diffusion distance of vertex i with respect to the boundary vertices l . More concretely, they prove that for solutions to boundary-constrained eigenvalue problems defined for certain Laplacians (e.g. absorbing random walk Laplacians), the diffusion distance from vertex i to the boundary, $d_l(i)$ satisfies the following inequality:

$$d_l(i) \log \left(\frac{1}{|1 - \lambda_1|} \right) \geq \log \left(\frac{2|u(i)|}{\|u\|_{L^\infty}} \right)$$

In other words, d_l is *highly correlated* with $|u|$. While Cheng et al. [14] derive this relationship explicitly for $|u_i|$, we empirically show that selecting vertices for active learning in this way performs poorly relative to state of the art methods. Inspired by recent sampling strategies for graph signal reconstruction [24] in the presence of noise, we demonstrate *reweighting* u_i^2 by \tilde{d}_i is an effective and principled heuristic. Additional details are provided in the supplemental material. Notably, we highlight that this score *comes at no extra computational cost* due to certain features of SSM—in particular SMM’s capability of producing estimates of the eigenvectors of L in addition to solutions of eq. (9).

Intuitively, the proposed score naturally encodes the eigenvector centrality and degree of a vertex as well as its geodesic distance to labeled vertices. In practice, we incorporate eigenvectors of higher order eigenvalues as well as interpolate towards a margin-based score as the label-rate increases, setting the score to:

$$s(v_i) = \|\tilde{d}_i \odot U_i^2\|_2,$$

where U is now an $n \times \ell$ matrix with eigenvectors as columns and U_i^2 denotes the matrix consisting of the square of the elements of column U_i . The choice of ℓ is left as a hyperparameter. In our experiments, we use $\ell = 3$.

Remark 4.1. If \mathcal{U}^c corresponds to the empty set, it is apparent that the smallest eigenvalue of $L_{\mathcal{U}} = \mathcal{L}$ is 0, and the corresponding eigenvector is $u = 1$. Hence, the acquisition score of each vertex is nothing but a constant times its degree.

While the work of Cheng et al. [14] provides concrete motivation for our method, we derive the following property that ensures samples are diverse, i.e. far from the labeled nodes.

Proposition 4.1. *Let N_i denote the neighborhood of vertex i . Consider score at vertex v_a , $s(v_a) = |u_i|$. For any connected pair of vertices v_a and v_b such that $v_a \notin N_s$, $v_b \in N_s$ for any $s \in \mathcal{U}$, there is a path from v_a to v_b such that the sequence of entries $(s(v_a), \dots, s(v_c), \dots, s(v_b))$ is nonincreasing.*

We provide an intuitive visualization of this score in Figure 2. The dataset is comprised of eight Gaussian clusters, each of equivalent size (300 samples), whose centers (i.e., means) lie evenly spaced apart on the unit circle. Each cluster is created by randomly sampling 300 points from a Gaussian with mean $\mu_i = (\cos(\pi i/4), \sin(\pi i/4))^T \in \mathbb{R}^2$ and standard deviation $\sigma_i = \sigma = 0.17$. The class structure is then assigned in an alternating fashion. For this example, efficient exploration via active learning is critical, particularly at low label rates. As we show in Figure 2 our score facilitates effective exploration of the geometric clustering structure—i.e. by sampling diversely from each cluster in the ring.

4.2 Complexity of active learning

We now comment on the time and space complexity of our algorithm. In general, one would assume that the most expensive step is computing the principal eigenpairs of $L_{\mathcal{U}}$. However, one key advantage of SSM is that it may provide accurate estimates of the principal eigenvectors of L , coinciding with the iterates X_t . In particular, $u = V\tilde{u}$ is an estimate for the eigenvectors of L , if \tilde{u} consists of the eigenvectors of \tilde{L} corresponding to the smallest two eigenvalues. Thus, when iteratively deriving vertices to label via active learning and subsequently solving the graph-based SSL classification problem, we may effectively re-use the previous iteration’s estimate of u to do active learning in linear time, comparable to simple, decision-boundary-based margin methods and far more efficient compared to uncertainty uncertainty-based techniques that necessitate full or partial eigenvector decompositions of dense covariance matrices.

5 Experiments

In this section, we present a numerical study of our algorithm applied to image classification in three domains at low label rates. We additionally explore medium and large label rates in comparison to recent state-of-the-art methods in the supplemental material.

First, we provide visualizations of predictions made by our proposed models in conjunction with Laplace learning. Note that a significant number of predictions made by Laplace Learning are concentrated around the origin.

In Figure 3, we present 2-d visualizations of the embeddings of our SSM and Procrustes initialization method in conjunction with those produced by Laplace Learning. Each plot is constructed by taking the embedding (used to make predictions) implied by Laplace Learning, our approximate method, or SSM and the value associated with class “2” on one axis and “7” on the other axis. Ideally, there should be a clear and distinct cluster structure associated with classes 2 and 7 around the supervised points and the rest of the digits. Clusture structure should also be associated with the barcode plots via a block diagonally dominant barcode. The key message is that SSM exhibits a strong capability to discriminate classes (i.e. a block diagonally dominant barcode) while respecting the geometry of the unlabeled examples. In contrast, embeddings produced by Laplace Learning are not discriminatory (i.e. the barcode is uniform) and the embeddings are degenerate—concentrated at a single point.

5.1 Experimental setup

We evaluated our method on three datasets: MNIST [30], Fashion-MNIST [47] and CIFAR-10 [29]. As in Calder et al. [12], we used pretrained autoencoders as feature extractors. For MNIST and Fashion-MNIST, we used variational autoencoders with 3 fully connected layers of sizes (784,400,20) and (784,400,30), respectively, followed by a symmetrically defined decoder. The autoencoder was trained for 100 epochs on each dataset. The autoencoder architecture, loss, and training are similar to Kingma and Welling [28].

For each dataset, we constructed a graph over the latent feature space. We used all available data to construct the graph, giving $n = 70,000$ nodes for MNIST and Fashion-MNIST, and $n = 60,000$

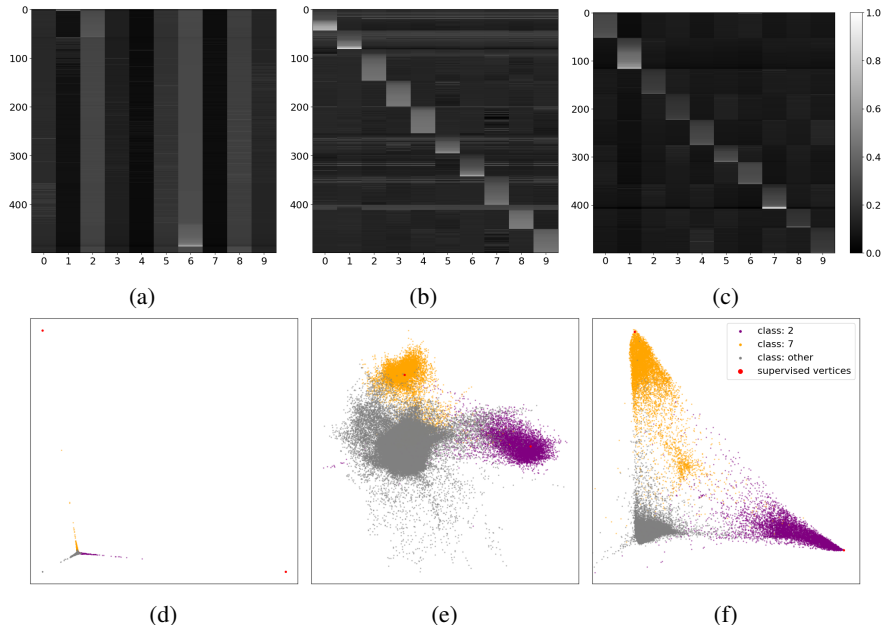


Figure 3: Barcode plots of MNIST predictors (left) and embeddings of samples for digits ‘2’ and ‘7’ (right). Learning is performed with 1 label per class. In the barcode plots, the rows are the samples, ordered by their class. Ordering of the columns was obtained by iteratively sorting the columns of the embedding matrices X . **(a,d)** Laplace learning exhibits degeneracy in the limit of unlabeled data. **(b,e)** Embeddings derived using Procrustes Analysis (Section 3.2) demonstrates no degeneracy but mixed samples from different classes together. **(c,f)** SSM exhibits good classification performance (a block diagonally dominant barcode) while respecting the geometry of unlabeled examples.

nodes for CIFAR-10. The graph was constructed as a K -nearest neighbor graph with Gaussian weights given by

$$w_{ij} = \exp(-4\|x_i - x_j\|^2/d_K(x_i)^2),$$

where x_i represents the latent variables for image i , and $d_K(x_i)$ is the distance in the latent space between x_i and its K^{th} nearest neighbor. We used $K = 10$ in all experiments. The weight matrix was then symmetrized by replacing W with $\frac{1}{2}(W + W^T)$.

In table 1, we compare our method to Laplace learning [56] and Poisson learning [12] as well as our refinement based on KL-partitioning to the PoissonMBO refinement. In the supplemental material, we compare our SSM approach and alignment-based approximation (Procrustes-SSL) against Laplace learning [56], Poisson learning [12], lazy random walks [52, 51], weighted nonlocal Laplacian (WNLL) [39], p -Laplace learning [16], and Laplacian Eigenmaps SSL (LE-SSL)[7]. Our SSM approach out-performs all methods in almost all cases.

5.2 Numerical results

Table 1 above and 2, 5, 4, and 6 in the supplementary show the average accuracy and standard deviation over all 100 trials for various label rates. Our SSM and SSM-KL methods consistently out-perform state-of-the-art. In particular, our method strictly improves over relevant methods on all datasets at a variety of label rates ranging from low (1 label) to high (4000). In the supplementary material, we expand on this evaluation—showing that the trend persists with medium label rate (100-1000 labels).

On all datasets, the proposed method exceeds the performance of related methods, particularly as the difficulty of the classification problem increases (i.e. CIFAR-10). In the supplementary material, we see that while Laplacian Eigenmaps SSL achieves better performance at higher label rates relative to Procrustes-SSL, at lower label rates Procrustes Analysis is significantly more accurate. We highlight the discrepancy between the approximate method (Procrustes-SSL) and our SSM-based refinement. This indicates the importance of SSM for recovering good critical points of eq. (9).

Table 1: Average accuracy over 100 trials with standard deviation in brackets. Best is bolded.

# FASHIONMNIST LABELS PER CLASS	1	2	3	4	5	4000
LAPLACE/LP [56]	18.4 (7.3)	32.5 (8.2)	44.0 (8.6)	52.2 (6.2)	57.9 (6.7)	85.8 (0.0)
POISSON [12]	60.8 (4.6)	66.1 (3.9)	69.6 (2.6)	71.2 (2.2)	72.4 (2.3)	81.1 (0.4)
SSM	61.2 (5.3)	66.4 (4.1)	70.3 (2.3)	71.6 (2.0)	73.2 (2.1)	86.1 (0.1)
POISSON-MBO [12]	62.0 (5.7)	67.2 (4.8)	70.4 (2.9)	72.1 (2.5)	73.1 (2.7)	86.8 (0.2)
SSM-KL	65.8 (1.1)	69.2 (1.2)	71.6 (1.2)	73.0 (0.4)	73.4 (0.3)	93.5 (0.1)
<hr/>						
# CIFAR-10						
LAPLACE/LP [56]	10.4 (1.3)	11.0 (2.1)	11.6 (2.7)	12.9 (3.9)	14.1 (5.0)	80.9 (0.0)
POISSON [12]	40.7 (5.5)	46.5 (5.1)	49.9 (3.4)	52.3 (3.1)	53.8 (2.6)	70.3 (0.9)
SSM	40.9 (6.1)	47.3 (5.9)	50.2 (4.3)	52.1 (4.3)	54.7 (3.4)	80.9 (0.1)
POISSON-MBO [12]	41.8 (6.5)	50.2 (6.0)	53.5 (4.4)	56.5 (3.5)	57.9 (3.2)	80.1 (0.3)
SSM-KL	43.7 (1.4)	51.4 (1.3)	54.1 (2.1)	57.1 (1.3)	58.8 (1.9)	83.9 (0.0)

We additionally evaluate the scaling behavior of our method at intermediate and high label rates. In Table 6 in the supplementary, we compare our method to Laplace learning and Poisson learning on MNIST and Fashion-MNIST with 500, 1000, 2000, and 4000 labels per class. We see significant degradation in the performance of Poisson Learning, however, our method maintains high-quality predictions in conjunction with Laplace learning. These results imply that while Laplace learning suffers degeneracy at low label rates and Poisson Learning seemingly degrades at large label rates, our framework performs reliably in both regimes—covering the spectrum of low and high supervised sampling rates. Furthermore, we highlight the practical efficacy of SSM in the appendix by comparing to existing standard open source implementations [44] of benchmark optimization algorithms [2].

5.3 Spectral algorithm for active learning

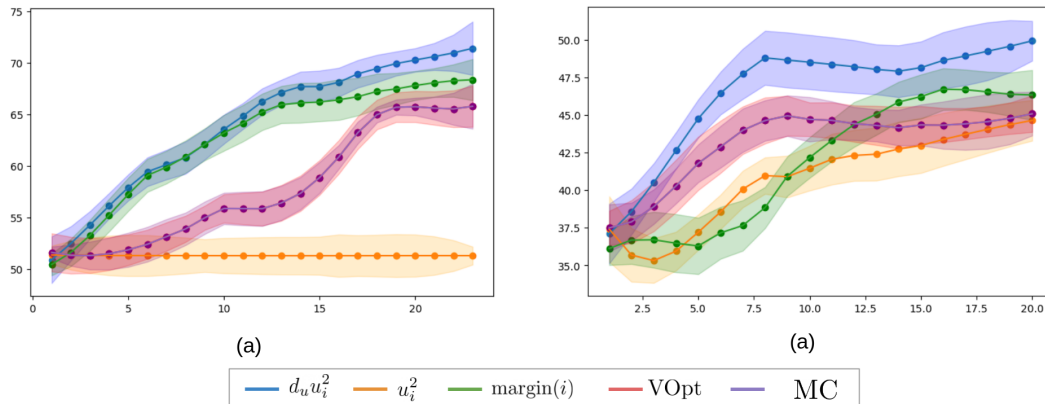


Figure 4: **Performance of SSM with active learning on F-MNIST (a) and CIFAR-10 (b)** Comparison between active learning methods using SSM-KL. X-axis denotes the number of vertices of the graph queries. Y-axis denotes the accuracy over 10-trials (initial labeled set). The shaded region denotes 0.5σ .

We numerically evaluate our selection scheme for active learning on FashionMNIST and CIFAR-10 in Figure 4. We compare to minimum margin-based uncertainty sampling [38], VOpt [25], and Model Change (MC) [33]. Note that uncertainty sampling selects query points according to the following notion of margin: $\text{margin}(i) = \arg \max_j (X_i)_j - \arg \max_{k \neq j} (X_i)_k$. One can interpret a smaller margin at a node as more uncertainty in the classification. We additionally note that MC and VOpt necessitate eigendecompositions of certain covariance matrices. Our score is implemented as

$$s'(v_i) = s(v_i) - \lambda_t \cdot \text{margin}(X),$$

where λ increases with t via $\lambda_{t+1} = (1 + \epsilon^{1/2k}) \lambda_t$ for some small value of $\epsilon = 10^{-4}$. We show that when coupled with the proposed SSM algorithm in an iterative our active learning scheme outperforms related methods at low-label rates across all benchmarks. We also emphasize that due to certain features of SSM, the computation of u_i is obtained for free after the first iteration.

6 Conclusion

We have proposed a novel formulation of semi supervised and active graph-based learning. Motivated by the robustness of semi-supervised Laplacian eigenmaps and spectral cuts in low label rate regimes, we introduced a formulation of Laplacian Eigenmaps with label constraints as a nonconvex Quadratically Constrained Quadratic Program. We have presented an approximate method as well as a generalization of a Sequential Subspace Method on the Stiefel Manifold. In a comprehensive numerical study on three image datasets, we have demonstrated that our approach consistently outperforms relevant methods with respect to semi-supervised accuracy in low, medium, and high label rate settings. We additionally demonstrate that selection of labeled vertices at low-label rates is critical. An active learning scheme is naturally derived from our formulation and we demonstrate it significantly improves performance, compared to competing methods. Future work includes a more rigorous analysis of the active learning score and of the problem in eq. (9) and our algorithmic generalization of SSM—for example, conditions on L and U that guarantee convergence to globally optimal solutions with convergence rates derived in Hager [21], Hager and Park [20], Absil et al. [2].

Acknowledgments and Disclosure of Funding

This work is partially supported by NSF-CCF-2217033.

References

- [1] P.-A. Absil and J. Malick. Projection-like retractions on matrix manifolds. *SIAM Journal on Optimization*, 22(1):135–158, 2012. doi: 10.1137/100802529. URL <https://doi.org/10.1137/100802529>.
- [2] P.-A. Absil, C. G. Baker, and K. A. Gallivan. Trust-region methods on Riemannian manifolds. *Found. Comput. Math.*, 7(3):303–330, July 2007. doi: 10.1007/s10208-005-0179-9.
- [3] P.-A. Absil, R. Mahony, and R. Sepulchre. *Optimization Algorithms on Matrix Manifolds*. Princeton University Press, USA, 2007. ISBN 0691132984.
- [4] A. E. K. Alaoui. Asymptotic behavior of ℓ_p -based laplacian regularization in semi-supervised learning. In *Annual Conference Computational Learning Theory*, 2016.
- [5] R. Ando and T. Zhang. Learning on graph with laplacian regularization. In B. Schölkopf, J. Platt, and T. Hoffman, editors, *Advances in Neural Information Processing Systems*, volume 19. MIT Press, 2006. URL <https://proceedings.neurips.cc/paper/2006/file/d87c68a56bc8eb803b44f25abb627786-Paper.pdf>.
- [6] A. Anis, A. Gadde, and A. Ortega. Efficient sampling set selection for bandlimited graph signals using graph spectral proxies. *IEEE Transactions on Signal Processing*, 64, 10 2015. doi: 10.1109/TSP.2016.2546233.
- [7] M. Belkin and P. Niyogi. Using manifold structure for partially labelled classification. In *Proceedings of the 15th International Conference on Neural Information Processing Systems*, NIPS’02, page 953–960, Cambridge, MA, USA, 2002. MIT Press.
- [8] M. Belkin and P. Niyogi. Laplacian eigenmaps for dimensionality reduction and data representation. *Neural Computation*, 15:1373–1396, 2003.
- [9] D. Bertsekas. *Nonlinear Programming*. Athena Scientific, 1999.
- [10] J. Calder. The game theoretic p-laplacian and semi-supervised learning with few labels. *Nonlinearity*, 32(1):301, dec 2018. doi: 10.1088/1361-6544/aae949. URL <https://dx.doi.org/10.1088/1361-6544/aae949>.
- [11] J. Calder. Consistency of lipschitz learning with infinite unlabeled data and finite labeled data. *SIAM Journal on Mathematics of Data Science*, 1(4):780–812, 2019. doi: 10.1137/18M1199241. URL <https://doi.org/10.1137/18M1199241>.

- [12] J. Calder, B. Cook, M. Thorpe, and D. Slepčev. Poisson learning: Graph based semi-supervised learning at very low label rates. In *Proceedings of the 37th International Conference on Machine Learning, ICML'20*. JMLR.org, 2020.
- [13] N. Cesa-Bianchi, C. Gentile, F. Vitale, and G. Zappella. Active learning on trees and graphs. *CoRR*, abs/1301.5112, 2013. URL <http://arxiv.org/abs/1301.5112>.
- [14] X. Cheng, M. Rachh, and S. Steinerberger. On the diffusion geometry of graph laplacians and applications. *Applied and Computational Harmonic Analysis*, 46(3):674–688, 2019. ISSN 1063-5203. doi: <https://doi.org/10.1016/j.acha.2018.04.001>. URL <https://www.sciencedirect.com/science/article/pii/S1063520318300745>.
- [15] A. R. Conn, N. I. M. Gould, and P. L. Toint. *Trust Region Methods*. Society for Industrial and Applied Mathematics, 2000. doi: 10.1137/1.9780898719857. URL <https://epubs.siam.org/doi/abs/10.1137/1.9780898719857>.
- [16] M. Flores, J. Calder, and G. Lerman. Analysis and algorithms for ℓ_p -based semi-supervised learning on graphs, 2019. URL <https://arxiv.org/abs/1901.05031>.
- [17] S. Gerschgorin. Über die abgrenzung der eigenwerte einer matrix. *Izvestija Akademii Nauk SSSR, Serija Matematika*, 7(3):749–754, 1931.
- [18] G. H. Golub and C. F. Van Loan. *Matrix Computations*. The Johns Hopkins University Press, third edition, 1996.
- [19] A. Guillory and J. A. Bilmes. Label selection on graphs. In Y. Bengio, D. Schuurmans, J. Lafferty, C. Williams, and A. Culotta, editors, *Advances in Neural Information Processing Systems*, volume 22. Curran Associates, Inc., 2009. URL https://proceedings.neurips.cc/paper_files/paper/2009/file/90794e3b050f815354e3e29e977a88ab-Paper.pdf.
- [20] W. Hager and S. Park. Global convergence of ssm for minimizing a quadratic over a sphere. *Math. Comput.*, 74:1413–1423, 07 2005. doi: 10.1090/S0025-5718-04-01731-4.
- [21] W. W. Hager. Minimizing a quadratic over a sphere. volume 12, 2001.
- [22] R. A. Horn and C. R. Johnson. *Matrix Analysis*. Cambridge University Press, Cambridge; New York, 2nd edition, 2013. ISBN 9780521839402.
- [23] M. Jacobs, E. Merkurjev, and S. Eshedoglu. Auction dynamics: A volume constrained mbo scheme. *Journal of Computational Physics*, 354:288–310, 2018. ISSN 0021-9991. doi: <https://doi.org/10.1016/j.jcp.2017.10.036>. URL <https://www.sciencedirect.com/science/article/pii/S0021999117308033>.
- [24] A. Jayawant and A. Ortega. A distance-based formulation for sampling signals on graphs. In *2018 IEEE International Conference on Acoustics, Speech and Signal Processing (ICASSP)*, pages 6318–6322, 2018. doi: 10.1109/ICASSP.2018.8461725.
- [25] M. Ji and J. Han. A variance minimization criterion to active learning on graphs. In N. D. Lawrence and M. Girolami, editors, *Proceedings of the Fifteenth International Conference on Artificial Intelligence and Statistics*, volume 22 of *Proceedings of Machine Learning Research*, pages 556–564, La Palma, Canary Islands, 21–23 Apr 2012. PMLR. URL <https://proceedings.mlr.press/v22/ji12.html>.
- [26] Y. Keller, R. R. Coifman, and S. Lafon. Data fusion and multicue data matching by diffusion maps. *IEEE Transactions on Pattern Analysis & Machine Intelligence*, 28(11):1784–1797, nov 2006. ISSN 1939-3539. doi: 10.1109/TPAMI.2006.223.
- [27] B. W. Kernighan and S. Lin. An efficient heuristic procedure for partitioning graphs. *The Bell System Technical Journal*, 49(2):291–307, 1970. doi: 10.1002/j.1538-7305.1970.tb01770.x.
- [28] D. P. Kingma and M. Welling. Auto-Encoding Variational Bayes. In *2nd International Conference on Learning Representations, ICLR 2014, Banff, AB, Canada, April 14-16, 2014, Conference Track Proceedings*, 2014.

- [29] A. Krizhevsky and G. Hinton. Learning multiple layers of features from tiny images. (0), 2009.
- [30] Y. Lecun, L. Bottou, Y. Bengio, and P. Haffner. Gradient-based learning applied to document recognition. *Proceedings of the IEEE*, 86(11):2278–2324, 1998. doi: 10.1109/5.726791.
- [31] J. Ma, Z. Ma, J. Chai, and Q. Mei. Partition-based active learning for graph neural networks. *Transactions on Machine Learning Research*, 2023. ISSN 2835-8856. URL <https://openreview.net/forum?id=e0xaRy1NuT>. Survey Certification.
- [32] U. Miekkala. Graph properties for splitting with grounded laplacian matrices. *BIT*, 33(3): 485–495, sep 1993. ISSN 0006-3835. doi: 10.1007/BF01990530. URL <https://doi.org/10.1007/BF01990530>.
- [33] K. Miller and A. L. Bertozzi. Model-change active learning in graph-based semi-supervised learning, 2021.
- [34] K. Miller and J. Calder. Poisson reweighted laplacian uncertainty sampling for graph-based active learning, 2022.
- [35] K. Miller, J. Mauro, J. Setiadi, X. Baca, Z. Shi, J. Calder, and A. L. Bertozzi. Graph-based active learning for semi-supervised classification of sar data, 2022.
- [36] B. Nadler, N. Srebro, and X. Zhou. Semi-supervised learning with the graph laplacian: The limit of infinite unlabelled data. In *Proceedings of the 22nd International Conference on Neural Information Processing Systems*, NIPS’09, page 1330–1338, Red Hook, NY, USA, 2009. Curran Associates Inc. ISBN 9781615679119.
- [37] J. Nocedal and S. J. Wright, editors. *Sequential Quadratic Programming*, pages 526–573. Springer New York, New York, NY, 1999. ISBN 978-0-387-22742-9. doi: 10.1007/0-387-22742-3_18. URL https://doi.org/10.1007/0-387-22742-3_18.
- [38] B. Settles. *Active Learning*. Synthesis Lectures on Artificial Intelligence and Machine Learning. Morgan & Claypool Publishers, 2012.
- [39] Z. Shi, S. Osher, and W. Zhu. Weighted nonlocal laplacian on interpolation from sparse data. *Journal of Scientific Computing*, 73(2-3), 4 2017. ISSN 0885-7474. doi: 10.1007/s10915-017-0421-z. URL <https://www.osti.gov/biblio/1537761>.
- [40] J. Silva, J. Marques, and J. a. Lemos. Selecting landmark points for sparse manifold learning. In Y. Weiss, B. Schölkopf, and J. Platt, editors, *Advances in Neural Information Processing Systems*, volume 18. MIT Press, 2005. URL https://proceedings.neurips.cc/paper_files/paper/2005/file/780965ae22ea6aee11935f3fb73da841-Paper.pdf.
- [41] D. Slepčev and M. Thorpe. Analysis of ℓ_1 -laplacian regularization in semisupervised learning. *SIAM Journal on Mathematical Analysis*, 51(3):2085–2120, 2019. doi: 10.1137/17M115222X. URL <https://doi.org/10.1137/17M115222X>.
- [42] D. C. Sorensen. Newton’s method with a model trust region modification. *SIAM Journal on Numerical Analysis*, 19(2):409–426, 1982. doi: 10.1137/0719026. URL <https://doi.org/10.1137/0719026>.
- [43] D. A. Spielman and S.-H. Teng. Nearly linear time algorithms for preconditioning and solving symmetric, diagonally dominant linear systems. *SIAM J. Matrix Anal. Appl.*, 35(3):835–885, jan 2014. ISSN 0895-4798.
- [44] J. Townsend, N. Koep, and S. Weichwald. Pymanopt: A python toolbox for optimization on manifolds using automatic differentiation. *J. Mach. Learn. Res.*, 17:137:1–137:5, 2016. URL <http://dblp.uni-trier.de/db/journals/jmlr/jmlr17.html#TownsendKW16>.
- [45] U. von Luxburg. A tutorial on spectral clustering. *CoRR*, abs/0711.0189, 2007. URL <http://arxiv.org/abs/0711.0189>.

- [46] C. Wang and S. Mahadevan. Manifold alignment using procrustes analysis. In *Proceedings of the 25th International Conference on Machine Learning, ICML '08*, page 1120–1127, New York, NY, USA, 2008. Association for Computing Machinery. ISBN 9781605582054. doi: 10.1145/1390156.1390297. URL <https://doi.org/10.1145/1390156.1390297>.
- [47] H. Xiao, K. Rasul, and R. Vollgraf. Fashion-mnist: a novel image dataset for benchmarking machine learning algorithms. *ArXiv*, abs/1708.07747, 2017.
- [48] H. Xu, H. Zha, R.-C. Li, and M. A. Davenport. Active manifold learning via gershgorin circle guided sample selection. In *AAAI Conference on Artificial Intelligence*, 2015.
- [49] X. Yang, H. Fu, H. Zha, and J. Barlow. Semi-supervised nonlinear dimensionality reduction. In *Proceedings of the 23rd International Conference on Machine Learning, ICML '06*, page 1065–1072, New York, NY, USA, 2006. Association for Computing Machinery. ISBN 1595933832. doi: 10.1145/1143844.1143978. URL <https://doi.org/10.1145/1143844.1143978>.
- [50] W. Zhang, S. Pan, S. Zhou, T. Walsh, and J. C. Weiss. Fairness amidst non-iid graph data: Current achievements and future directions, 2023.
- [51] D. Zhou, O. Bousquet, T. N. Lal, J. Weston, and B. Schölkopf. Learning with local and global consistency. In *NIPS*, 2003.
- [52] D. Zhou, B. Schölkopf, C. Rasmussen, H. Bühlhoff, and M. Giese. Learning from labeled and unlabeled data using random walks. volume 3175, 08 2004. ISBN 978-3-540-22945-2. doi: 10.1007/978-3-540-28649-3_29.
- [53] D. Zhou, J. Huang, and B. Schölkopf. Learning from labeled and unlabeled data on a directed graph. In *Proceedings of the 22nd International Conference on Machine Learning, ICML '05*, page 1036–1043, New York, NY, USA, 2005. Association for Computing Machinery. ISBN 1595931805. doi: 10.1145/1102351.1102482. URL <https://doi.org/10.1145/1102351.1102482>.
- [54] X. Zhou and M. Belkin. Semi-supervised learning by higher order regularization. In G. Gordon, D. Dunson, and M. Dudík, editors, *Proceedings of the Fourteenth International Conference on Artificial Intelligence and Statistics*, volume 15 of *Proceedings of Machine Learning Research*, pages 892–900, Fort Lauderdale, FL, USA, 11–13 Apr 2011. PMLR. URL <https://proceedings.mlr.press/v15/zhou11b.html>.
- [55] X. Zhou and N. Srebro. Error analysis of laplacian eigenmaps for semi-supervised learning. In G. Gordon, D. Dunson, and M. Dudík, editors, *Proceedings of the Fourteenth International Conference on Artificial Intelligence and Statistics*, volume 15 of *Proceedings of Machine Learning Research*, pages 901–908, Fort Lauderdale, FL, USA, 11–13 Apr 2011. PMLR. URL <https://proceedings.mlr.press/v15/zhou11c.html>.
- [56] X. Zhu, Z. Ghahramani, and J. Lafferty. Semi-supervised learning using gaussian fields and harmonic functions. In *Proceedings of the Twentieth International Conference on International Conference on Machine Learning, ICML '03*, page 912–919. AAAI Press, 2003. ISBN 1577351894.
- [57] X. J. Zhu. Semi-supervised learning literature survey. Technical report, University of Wisconsin-Madison Department of Computer Sciences, 2005.

Overview of supplemental material. In Section A, we provide additional numerical evidence for the efficacy of our framework compared to a larger variety of methods for graph-based semi-supervised learning. We also explore the effect of the label rate at a higher resolution and compare our proposed SSM algorithm to existing open-source implementations of classic algorithms for Riemannian optimization. In Section B, we discuss an alternative perspective of our active learning score. This alternative perspective is inspired by recent literature on noise-robust sampling techniques developed in the context of graph signal processing. We derive a lower-bound on the smallest eigenvalue of $L_{\mathcal{U}}$ and demonstrate that our score is a good proxy for this bound. This implication of this bound is that our algorithm can be interpreted a greedy algorithm for degree-weighted uncertainty sampling that is robust to any underlying noise in the data or graph construction. In Section C, we provide a theoretical analysis of SSM with the goal of developing a convergence result for the algorithm. We conclude the supplemental material in Section D by discussing the limitations of our work and the broader societal impact of graph-based semi-supervised learning.

A Additional Results

Here, we provide additional numerical evidence for the efficacy of our framework, compared to a larger variety of graph-based semi-supervised learning algorithms.

A.1 Benchmarking graph-based semi-supervised learning algorithms

In this section, we provide extended results on our proposed methods. First, we present average accuracy scores over additional label rates on MNIST, Fashion MNIST, and CIFAR-10. We compare our SSM approach and alignment-based approximation presented in section 3.2 (Procrustes-SSL) against Laplace learning [56], Poisson learning [12], lazy random walks [52, 51], weighted nonlocal Laplacian (WNLL) [39], p -Laplace learning [16], and Laplacian Eigenmaps SSL (LE-SSL)[7]. We restrict our comparison to methods *without additional cut-based refinement* (e.g. PoissonMBO or KL), which we provide in the following table.

We conduct additional experiments to compare Procrustes-SSL + MBO, SSM + MBO, PoissonMBO, VolumeMBO at low (1, 3, 5) and high (4000) label-rates. Importantly, to conduct a fair comparison, we have augmented our proposed methods with the MBO-based refinement procedure proposed in Sec 2.4 of Calder et al. [12] with the same set of parameters. This amounts to replacing the PoissonLearning step (line 3, Algorithm 2 of Calder et al. [12]) with either of our proposed methods (Procrustes-SSL or SSM). We show that when our method is augmented with this additional refinement step, we gain significant improvements in solution quality as well as smaller standard deviation while outperforming all MBO-based approaches. This trend notably persists through the high-label-rate regime.

Next, we evaluate the ability of our approach to retain strong predictive performance at medium and high label rates. Here, we show that Poisson Learning fails to retain superior results as compared to Laplace Learning.

Table 2: MNIST: Average accuracy over 100 trials with standard deviation in brackets. Best is bolded.

# LABELS PER CLASS	1	2	3	4	5
LAPLACE/LP [56]	16.1 (6.2)	28.2 (10.3)	42.0 (12.4)	57.8 (12.3)	69.5 (12.2)
NEAREST NEIGHBOR	55.8 (5.1)	65.0 (3.2)	68.9 (3.2)	72.1 (2.8)	74.1 (2.4)
RANDOM WALK [52]	66.4 (5.3)	76.2 (3.3)	80.0 (2.7)	82.8 (2.3)	84.5 (2.0)
WNLL [39]	55.8 (15.2)	82.8 (7.6)	90.5 (3.3)	93.6 (1.5)	94.6 (1.1)
P-LAPLACE [16]	72.3 (9.1)	86.5 (3.9)	89.7 (1.6)	90.3 (1.6)	91.9 (1.0)
POISSON [12]	90.2 (4.0)	93.6 (1.6)	94.5 (1.1)	94.9 (0.8)	95.3 (0.7)
LE-SSL [7]	43.1 (0.2)	87.4 (0.1)	88.2 (0.0)	90.5 (0.1)	93.7 (0.0)
PROCRUSTES-SSL	87.0 (0.1)	89.1 (0.0)	89.1 (0.0)	89.6 (0.1)	91.4 (0.0)
SSM	90.6 (3.8)	94.1 (2.1)	94.7 (1.6)	95.1 (1.1)	96.3 (0.9)

Table 3: FashionMNIST: Average accuracy scores over 100 trials with standard deviation in brackets.

# LABELS PER CLASS	1	2	3	4	5
LAPLACE/LP [56]	18.4 (7.3)	32.5 (8.2)	44.0 (8.6)	52.2 (6.2)	57.9 (6.7)
NEAREST NEIGHBOR	44.5 (4.2)	50.8 (3.5)	54.6 (3.0)	56.6 (2.5)	58.3 (2.4)
RANDOM WALK [52]	49.0 (4.4)	55.6 (3.8)	59.4 (3.0)	61.6 (2.5)	63.4 (2.5)
WNLL [39]	44.6 (7.1)	59.1 (4.7)	64.7 (3.5)	67.4 (3.3)	70.0 (2.8)
P-LAPLACE [16]	54.6 (4.0)	57.4 (3.8)	65.4 (2.8)	68.0 (2.9)	68.4 (0.5)
POISSON [12]	60.8 (4.6)	66.1 (3.9)	69.6 (2.6)	71.2 (2.2)	72.4 (2.3)
LE-SSL [7]	22.0 (0.1)	51.3 (0.1)	62.0 (0.0)	65.4 (0.0)	63.2 (0.0)
PROCRUSTES-SSL	50.1 (0.1)	55.6 (0.1)	62.0 (0.0)	63.4 (0.0)	61.3 (0.0)
SSM	61.2 (5.3)	66.4 (4.1)	70.3 (2.3)	71.6 (2.0)	73.2 (2.1)
# LABELS PER CLASS	10	20	40	80	160
LAPLACE/LP [56]	70.6 (3.1)	76.5 (1.4)	79.2 (0.7)	80.9 (0.5)	82.3 (0.3)
NEAREST NEIGHBOR	62.9 (1.7)	66.9 (1.1)	70.0 (0.8)	72.5 (0.6)	74.7 (0.4)
RANDOM WALK [52]	68.2 (1.6)	72.0 (1.0)	75.0 (0.7)	77.4 (0.5)	79.5 (0.3)
WNLL [39]	74.4 (1.6)	77.6 (1.1)	79.4 (0.6)	80.6 (0.4)	81.5 (0.3)
P-LAPLACE [16]	73.0 (0.9)	76.2 (0.8)	78.0 (0.3)	79.7 (0.5)	80.9 (0.3)
POISSON [12]	75.2 (1.5)	77.3 (1.1)	78.8 (0.7)	79.9 (0.6)	80.7 (0.5)
LE-SSL [7]	67.1 (0.0)	68.8 (0.0)	70.5 (0.0)	70.9 (0.0)	66.6 (0.0)
PROCRUSTES-SSL	65.3 (0.0)	66.2 (0.0)	68.3 (0.0)	69.6 (0.0)	64.5 (0.0)
SSM	76.4 (1.4)	78.1 (1.3)	79.4 (0.9)	80.3 (0.7)	82.6 (0.4)

Table 4: CIFAR-10: Average accuracy scores over 100 trials with standard deviation in brackets.

# LABELS PER CLASS	1	2	3	4	5
LAPLACE/LP [56]	10.4 (1.3)	11.0 (2.1)	11.6 (2.7)	12.9 (3.9)	14.1 (5.0)
NEAREST NEIGHBOR	31.4 (4.2)	35.3 (3.9)	37.3 (2.8)	39.0 (2.6)	40.3 (2.3)
RANDOM WALK [52]	36.4 (4.9)	42.0 (4.4)	45.1 (3.3)	47.5 (2.9)	49.0 (2.6)
WNLL [39]	16.6 (5.2)	26.2 (6.8)	33.2 (7.0)	39.0 (6.2)	44.0 (5.5)
P-LAPLACE [16]	26.0 (6.7)	35.0 (5.4)	42.1 (3.1)	48.1 (2.6)	49.7 (3.8)
POISSON [12]	40.7 (5.5)	46.5 (5.1)	49.9 (3.4)	52.3 (3.1)	53.8 (2.6)
LE-SSL [7]	16.2 (0.1)	36.5 (0.1)	44.4 (0.1)	43.0 (0.0)	46.1 (0.0)
PROCRUSTES-SSL	36.2 (0.1)	40.6 (0.1)	44.8 (0.1)	42.9 (0.0)	45.6 (0.0)
SSM	40.9 (6.1)	47.3 (5.9)	50.2 (4.3)	52.1 (4.3)	54.7 (3.4)
# LABELS PER CLASS	10	20	40	80	160
LAPLACE/LP [56]	21.8 (7.4)	38.6 (8.2)	54.8 (4.4)	62.7 (1.4)	66.6 (0.7)
NEAREST NEIGHBOR	43.3 (1.7)	46.7 (1.2)	49.9 (0.8)	52.9 (0.6)	55.5 (0.5)
RANDOM WALK [52]	53.9 (1.6)	57.9 (1.1)	61.7 (0.6)	65.4 (0.5)	68.0 (0.4)
WNLL [39]	54.0 (2.8)	60.3 (1.6)	64.2 (0.7)	66.6 (0.6)	68.2 (0.4)
P-LAPLACE [16]	56.4 (1.8)	60.4 (1.2)	63.8 (0.6)	66.3 (0.6)	68.7 (0.3)
POISSON [12]	58.3 (1.7)	61.5 (1.3)	63.8 (0.8)	65.6 (0.6)	67.3 (0.4)
LE-SSL [7]	47.9 (0.0)	50.4 (0.0)	46.5 (0.0)	45.0 (0.0)	46.7 (0.0)
PROCRUSTES-SSL	46.1 (0.0)	50.0 (0.0)	46.9 (0.0)	45.5 (0.0)	46.9 (0.0)
SSM	59.4 (2.3)	62.4 (1.7)	64.9 (1.1)	66.6 (0.4)	68.4 (0.4)

A.2 Comparison with an open-source tool for Riemannian optimization

Additionally, we include a comparison between the SSM component of our framework and the general first (RG) and second-order (TR) Riemannian optimization algorithms implemented in the Pymanopt package [44]. For submanifolds of Euclidean spaces, first-order methods for constrained problems that consist of iteratively taking a tangent step in the Euclidean space followed by a projection (i.e. our projected gradient method) are functionally equivalent to Riemannian Gradient methods [3, 1].

Table 5: Additional results comparing KL and MBO schemes at low and medium-high label rates.

MNIST # LABELS PER CLASS	1	3	5	4000
POISSONMBO [12]	96.5 (2.6)	97.2 (0.1)	97.2 (0.1)	97.3 (0.0)
VOLUMEMBO [23]	89.9 (7.3)	96.2 (1.2)	96.7 (0.6)	96.9 (0.1)
PROCRUSTES-SSL + MBO	94.1 (0.1)	96.0 (0.0)	97.1 (0.0)	97.2 (0.0)
SSM + MBO	97.6 (0.1)	97.6 (0.1)	97.6 (0.1)	99.1 (0.0)
SSM-KL	97.6 (0.1)	97.6 (0.1)	97.6 (0.1)	99.1 (0.0)

FASHIONMNIST # LABELS PER CLASS	1	3	5	4000
POISSONMBO [12]	62.0 (5.7)	70.4 (2.9)	73.1 (2.7)	86.8 (0.2)
VOLUMEMBO [23]	54.7 (5.2)	66.1 (3.3)	70.1 (7.1)	85.5 (0.2)
PROCRUSTES-SSL + MBO	53.6 (2.8)	60.3 (4.6)	66.5 (3.2)	70.1 (0.0)
SSM + MBO	65.3 (1.9)	71.4 (1.3)	73.2 (0.6)	93.4 (0.1)
SSM-KL	65.8 (1.1)	71.6 (1.2)	73.4 (0.3)	93.5 (0.1)

CIFAR-10 # LABELS PER CLASS	1	3	5	4000
POISSONMBO [12]	41.8 (6.5)	53.5 (4.4)	57.9 (3.2)	80.1 (0.3)
VOLUMEMBO [23]	38.0 (7.2)	50.1 (5.7)	55.3 (3.8)	75.1 (0.2)
PROCRUSTES-SSL + MBO	38.1 (4.7)	42.6 (3.3)	46.4 (2.9)	54.1 (0.1)
SSM + MBO	42.3 (1.5)	53.9 (2.5)	57.9 (2.1)	83.7 (0.0)
SSM-KL	43.7 (1.4)	54.1 (2.1)	58.8 (1.9)	83.9 (0.0)

Table 6: Scaling behavior as the number of labeled vertices increases beyond the low label rate regime: Average accuracy scores over 10 trials. Standard deviation across trials approaches zero for all methods. We use the publicly available implementation of Poisson Learning [11].

# LABELS PER CLASS	500	1000	2000	4000
MNIST				
LAPLACE/LP	97.8	97.9	98.1	98.3
POISSON	97.1	96.9	96.3	93.8
SSM	97.8	98.0	98.1	98.2
FASHIONMNIST				
LAPLACE/LP	84.0	84.7	85.3	85.8
POISSON	82.2	78.9	74.9	58.6
SSM	84.3	84.8	85.9	86.1

Table 7: Tool comparison: wall time per-iteration, # iterations to reach $|\text{grad}| \leq 10e-5$ (– denotes no convergence), and accuracy using MNIST digits restricted to 0-5 with 1 label / class.

	WALL TIME / ITER	# ITER TO CRIT. POINT	ACCURACY
SSM	6.1	7	0.99
TR	145.5	10	0.94
RG	3.4	–	0.75

In our work, we consider the Euclidean Projection onto the Stiefel manifold given by the SVD. However, Pymanopt by default defines the retraction via the QR decomposition (although SVD-based retractions are also supported). In theory, this should yield similar convergence results in theory and practice.

We also consider the second-order trust-region method supported by Pymanopt [2]. We note that one contribution of our work is the extension of SSM, a state of the art method for large-scale trust-region subproblems to more general QCQPs. More generally, our generalization and application of SSM is motivated by its success on large scale trust-region subproblems (which our problem shares many characteristics with) - with remarkable empirical results and robust convergence guarantees, even for so-called “degenerate problems”. SSM has many advantages over typical methods for Riemannian optimization (including first and second-order trust-region methods). To summarize, we claim that

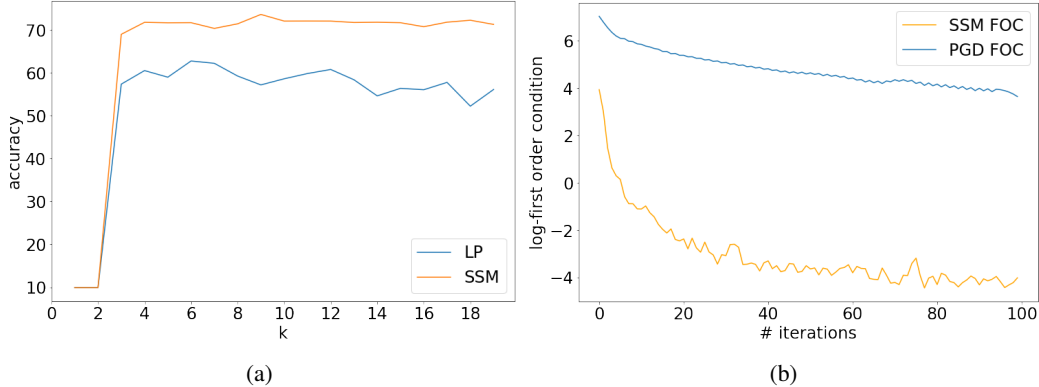


Figure 5: **Robust performance of SSM on F-MNIST.** (a) robustness to different numbers of neighbors k used to construct the graph, averaged over 10 trials, 5 labels per-class. (b) The log-first order condition, i.e. empirical rate of convergence of Projected gradient method and SSM on F-MNIST with 5 labels per-class.

our proposed SSM method + Procrustes initialization, designed specifically for the problem we propose should outperform the more general techniques implemented in Pymanopt.

We show in Fig. 5b that the choice of subspaces play a critical role in the rate and quality of convergence of our method (compared to first-order methods). One may also ask how our method compares to traditional second-order methods (e.g. Riemannian Trust-region). In theory, SSM employs a special set of vectors to estimate the Hessian information to update the search direction via subspace minimization. As a result, the Hessian information estimated from SSM is usually better than the Hessian estimated from CG or BFGS methods typically used for trust-region type approaches.

Figure 5a shows the accuracy of SSM at 5 labels per class as a function of the number of neighbors K used in constructing the graph, showing that the algorithm is not significantly sensitive to this choice.

In Figure 5b, we demonstrate the convergence behavior of SSM and the projected gradient method discussed previously by plotting the norm of the first order condition (FOC): $\|LX_tC - BC^{1/2} - X_t\Lambda_t\|$. Note that while both methods are guaranteed to monotonically reduce the objective of eq. (9) via line search, SSM rapidly converges to a critical point, while the projected gradient method fails to converge, even after 100 iterations.

B Graph-Based Active Learning

In this section, we provide additional justification for the sampling score proposed in the main text. As mentioned in the main text, the component of score involving the eigenvector of $L_{\mathcal{U}}$ associated with the smallest eigenvalue is motivated primarily by previous work that investigates features encoded by the eigenvectors of the Laplacian of a graph with grounded vertices [14]. These features specifically facilitate efficient methods to diversely sample the graph. Additionally, our score has connections to the graph signal processing literature [24, 6] which aims to robustly recover a graph signal by sampling a sparse set of vertices. It has been demonstrated that one ideal sampling strategy that is robust to noise aims to maximize the smallest eigenvalue of the principal submatrix of the Laplacian, analogous to $L_{\mathcal{U}}$. Below, we demonstrate that our method, namely squaring the entries of u and weighting by \tilde{d}_i , is directly related to one lower bound of the smallest eigenvalue of $L_{\mathcal{U}}$.

B.0.1 Lower bound estimate for eigenvalues of $L_{\mathcal{U}}$

Consider a grounded Laplacian $L_{\mathcal{U}}$ and the associated perturbation implied by labeling a vertex $E^i = \sum_{j \in \mathcal{U}} A_{ij}(E_{ij} + E_{ji})$, where E_{ij} is an $n \times n$ matrix with $(L_{\mathcal{U}})_{ij}$ in the ij -th position (and, to be clear, A_{ij} is a scalar). Let u be one eigenvector of $L_{\mathcal{U}}$. Then, we have that the bound essentially follows from a proof of Weyl's inequality [22]. If G is connected or $|\mathcal{U}^c| > 0$, the eigenvectors of $L_{\mathcal{U}}$ form a basis for \mathbb{R}^n . Let v be a unit eigenvector of $L_{\mathcal{U}} - E^i$ with eigenvector decomposition (where

$u^{(j)}$ is the eigenvector associated with the j -th eigenvalue of $L_{\mathcal{U}}$).

$$v = \sum_{j=1}^n t_j u^{(j)}$$

for some coefficients t_j s.t. $\sum_j t_j^2 = 1$. Then the eigenvalue λ' of $L_{\mathcal{U}} - E^i$ is

$$\lambda' = v^\top (L_{\mathcal{U}} - E^i) v = \sum_{j=1}^n t_j^2 (\lambda_j - \langle u^{(j)}, E^i u^{(j)} \rangle) \geq \min_{j=1, \dots, n} \{ \lambda_j - \langle u^{(j)}, E^i u^{(j)} \rangle \} \quad (17)$$

Thus, the maximum perturbation of the smallest eigenvalue of $L_{\mathcal{U}} - E^i$ is bounded below by the largest eigenvalue of E^i (recall that E^i has nonzero entries associated with the i -th column and i -th row of $L_{\mathcal{U}}$). Hence, to increase the eigenvalue of $L_{\mathcal{U}}$, a greedy selection implies the choice of i that maximizes $-\langle u^{(j)}, E^i u^{(j)} \rangle = 2u_i^{(j)} \sum_{k \in \mathcal{U}} A_{ij} u_k^{(j)}$.

Note that when the spectral gap of $L_{\mathcal{U}}$ is large, j need not be taken over $[n]$. More concretely, suppose $\lambda_{k'+1} - \lambda_1 > \epsilon$, where ϵ is the largest eigenvalue of $\{E^i : i = 1, \dots, n\}$. Note that $\lambda' \geq \lambda$. Then,

$$\lambda' \geq \min \left\{ \min_{j=1, \dots, k'} \{ \lambda_j - \langle u^{(j)}, E^i u^{(j)} \rangle \}, \lambda_{k'+1} - \epsilon \right\} \geq \min_{j=1, \dots, k'} \{ \lambda_j - \langle u^{(j)}, E^i u^{(j)} \rangle \} \quad (18)$$

We highlight that the spectral gap of graph Laplacians of graphs constructed on data, particularly KNN graphs, exhibit fast growth of the eigenvalues [45, 26] and large spectral gaps. On such graphs, the low-frequency eigenvectors (eigenvectors corresponding to the smallest eigenvalues of the Laplacian) are “smooth” over the graph and the score presented in the main text is a good proxy for the above bound, i.e. $2u_i^{(j)} \sum_{k \in \mathcal{U}} A_{ij} u_k^{(j)} \approx 2\tilde{d}_i (u_i)^2$. As we show below, using the ranking implied by *just* u_i corresponds to a diversity selection strategy that iteratively selects vertices that are far from the set of labeled nodes. Intuitively, weighting this measure by \tilde{d}_i encourages selection of vertices that are *well connected*. Experimentally, as shown in the main text, this also has the effect of improving results.

B.1 Spectral active learning score

For the purposes of this section, we will consider a slightly different scoring function than the one presented in the main text. Let $s(v_i) = |u_i|$, where u_i is the i -th component of the eigenvector of $L_{\mathcal{U}}$ corresponding to the smallest eigenvalue of $L_{\mathcal{U}}$. Note that when the graph is connected, from the Perron-Frobenius theorem [32, 22], the eigenvector associated with the smallest eigenvalue of $L_{\mathcal{U}}$ can be chosen to be elementwise nonnegative.

Proposition B.1. *Let N_i denote the neighborhood of vertex i . Consider the score at vertex v_a , $s(v_a) = |u_i|$. For any connected pair of vertices v_a and v_b such that $v_a \notin N_k$, $v_b \in N_k$ for any $k \in \mathcal{U}^c$, there is a path from v_a to v_b such that the sequence of entries $(s(v_a), \dots, s(v_c), \dots, s(v_b))$ is nonincreasing.*

Proof. We will consider a vertex v_i and its score $s(v_i)$ when its neighborhood does not contain a labeled vertex and its score $s'(v_i)$ when its neighborhood does contain a labeled vertex, v_ℓ . First, note that the i th entry of the eigenvectors of $L_{\mathcal{U}}$ are characterized by the system

$$d_i u_i - \sum_{v_j \in \mathcal{U}} A_{ij} u_j = \lambda u_i.$$

Then, write $u_i = \frac{\sum_{v_j \in \mathcal{U}} A_{ij} u_j}{d_i - \lambda}$ and consider labeling a single neighbor v_ℓ in the neighborhood of v_i :

$$s(v_i) = |u_i| = \left| \frac{\sum_{j \in \mathcal{U}} A_{ij} u_j}{d_i - \lambda} \right| = \frac{\sum_{j \in \mathcal{U}} A_{ij} |u_j|}{|d_i - \lambda|} \quad (19)$$

$$\geq \frac{\sum_{j \in \mathcal{U}} A_{ij} |u_j| - |u_\ell|}{|d_i - \lambda|} = \left| \frac{\sum_{j \in \mathcal{U} \setminus \{u_\ell\}} A_{ij} u_j}{d_i - \lambda} \right| \quad (20)$$

$$= s'(v_i) \quad (21)$$

Naturally, the implication is that the score of a vertex decreases as its neighbors are labeled. Furthermore we have that

$$s(v_i) = |u_i| = \left| \frac{\sum_{j \in \mathcal{U}} A_{ij} u_j}{d_i - \lambda} \right| \geq \frac{1}{d_i} \left| \sum_{j \in \mathcal{U}} A_{ij} u_j \right| = \frac{1}{d_i} \sum_{j \in \mathcal{U}} A_{ij} s(v_j) \quad (22)$$

Thus, the score of a vertex v_i is greater than the average score of its neighbors, and therefore, there must be a neighbor of v_i with score less than $s(v_i)$. Since each vertex has a neighbor with smaller score, starting from any vertex there is a path consisting of vertices that have decreasing scores that must finish at a vertex with neighbor in \mathcal{U}^c . \square

Again, we emphasize that this is not necessarily true when $|u_i|$ is weighted by the degree \tilde{d}_i . Including this weight is intuitively motivated by the principle of connectedness. In other words, our score selects vertices *that are both distant from the set of labeled vertices, and well-connected*.

C Convergence of SSM and Additional Computational Results

C.1 Preliminaries

$$\min_{X: X \in \text{St}(n, k)} \langle X, LXC \rangle - \langle X, BC^{1/2} \rangle \quad (23)$$

Quadratic minimization over the Stiefel manifold is a generalization of the well-known nonconvex quadratic over the unit ball or sphere. These problems often arise in trust region methods [42, 15]. Notably, there could exist many local solutions in 23. We will demonstrate convergence to critical points of two iterative methods: a gradient projection method and the Sequential Subspace Method proposed in this work. Furthermore, when the subspaces component to the SSM algorithm contain the span of the first k nontrivial eigenvectors of L , we show that the quality of the stationary point is characterized by the eigenvalues of the Lagrange multipliers Λ .

First denote the the eigenvector decomposition of L be given by

$$L = [v_1, v_2, \dots, v_n] \text{diag}(d_1, \dots, d_n) [v_1, v_2, \dots, v_n]^T$$

To summarize, we will show the following:

- We propose a gradient projection method to solve 23. We prove convergence with the Armijo rule in Prop. C.7.
- We analyze the proposed iterative method in the framework of SSM, constructing a sequence of subspaces to reach one approximation of local solutions, where the subspace consists of columns of X_t , $LX_t C - BC^{1/2}$ and eigenvectors associated with d_i , $i = 1, \dots, k$. Each sub-problem can be solved by the aforementioned gradient projection method. We demonstrate global convergence to high-quality critical points. Theoretically, when $C = I$ and the multiplicity of the first nontrivial eigenvalue is greater than or equal to k , a local solution is actually a global solution. However, we leave this analysis as future work.

First, we review some known results in the spherical case, i.e., $\text{St}(n, 1)$. Next, we derive convergence of a projected gradient method to solutions satisfying the first order condition eq. (11). Finally, Theorem 1 states the convergence of SSM to a high-quality local solution is guaranteed.

C.1.1 Notation

We assume k is a positive integer (much) less than n . Let K denote the set $\{1, 2, \dots, k\}$. Let $I_{n,k}$ denote the sub matrix of the identity matrix I_n , consisting of the first k columns. Let O_k be the orthogonal group, i.e., $Q \in O_k$ if and only if $Q \in \mathbb{R}_{k,k}$ and $Q^T Q = I_k$.

C.2 Preliminary results in the spherical case

eq. (23) is one natural generalization of the constrained problem [21, 20]

$$\min_x \{x^T A x - 2\langle x, b \rangle : \|x\| = 1, x \in \mathbb{R}^n\} \quad (24)$$

This problem is related to the trust region subproblem:

$$\min_x \{x^\top Ax - 2\langle x, b \rangle : \|x\| \leq 1, x \in \mathbb{R}^n\} \quad (25)$$

The following two propositions describe the global solution of 24. See [42]. The condition 26 states that the global solution x is the critical point associated with λ bounded above by the smallest eigenvalue d_1 of A .

Proposition C.1 (Hager and Park [20]). *A vector $x \in \mathbb{R}^n$ is a global solution of 24, if and only if $\|x\| = 1$, and*

$$A - \lambda I \succcurlyeq 0, \quad (A - \lambda I)x = b \quad (26)$$

holds for some $\lambda \in \mathbb{R}$

Proposition C.2 (Hager [21]). *Consider the eigenvector decomposition*

$$A = [v_1, v_2, \dots, v_n] \text{diag}(d_1, \dots, d_n) [v_1, v_2, \dots, v_n]^\top.$$

Let V_1 be the matrix whose columns are eigenvectors of L with eigenvalue d_1 . Then, $x = Vc$ is a solution for a vector c chosen in the following way:

- *Degenerate case: suppose $V_1^\top b = 0$ and $c_\perp := \|(A - d_1 I)^\dagger b\| \leq 1$. Then, $\lambda = d_1$ and $x = (1 - c_\perp^2)^{1/2} v_1 + (A - d_1 I)^\dagger b$*
- *Nondegenerate case: $\lambda < d_1$ is chosen so that $x = (A - \lambda I)^{-1} b$ with $\|x\| = 1$.*

Remark C.1 (Hager and Park [20]). Note that $\|(A - \lambda I)^{-1} b\|$ decreases monotonically with respect to $\lambda \leq d_1$. A proper value of λ meets the condition $\|x\| = 1$. A tighter bound on λ can be estimated from

$$(d_1 - \lambda) \|V_1 b\|^2 \leq 1 = \|(A - \lambda I)^{-1} b\|^2 \leq (d_1 - \lambda)^{-2} \|b\|^2$$

With $\|V_1 b\| > 0$, λ lies in the interval $[d_1 - \|b\|, d_1 - \|V_1 b\|]$

C.3 Computational results

In this section, we provide the precise computations involved in the derivation of eq. (9) from eq. (7).

C.3.1 Derivation of B and C

Given $\mathbf{1}^\top X = 0$ and $X^\top X = pI$, we have that $\mathbf{1}^\top X_u = -r^\top$ and $X_u^\top X_u = pI - X_l^\top X_l = (p - \tilde{p})I$, where $r = \mathbf{1}^\top X_l$.

Let $(\tilde{X}_u)_i = (X_u)_i + \frac{1}{n} r$. We have the following:

1. $\mathbf{1}^\top \tilde{X}_u = 0$
2. $X_u^\top X_u = \tilde{X}_u^\top \tilde{X}_u + \frac{1}{n} r^\top r$

Thus, $\tilde{X}_u^\top \tilde{X}_u = (p - \tilde{p})I - \frac{1}{n} r^\top r$

Consider $\langle X_0, LX_0 \rangle = X_u^\top L_u X_u + 2X_u^\top L_{ul} X_l + X_l^\top L_l X_l$. Let $R = \frac{1}{n} \begin{bmatrix} r^\top \\ \vdots \\ r^\top \end{bmatrix} \in \mathbb{R}^{n \times k}$. We have that

$$\begin{aligned} \langle X_0, LX_0 \rangle &= \tilde{X}_u^\top L_u \tilde{X}_u - 2\tilde{X}_u^\top L_u R \\ &\quad + R^\top L_u R + 2\tilde{X}_u^\top L_{ul} X_l - 2R^\top L_{ul} X_l + X_l^\top L_l X_l \\ &= \tilde{X}_u^\top L_u \tilde{X}_u + 2\tilde{X}_u^\top (-L_u R + L_{ul} X_l) \\ &\quad + R^\top L_u R - 2R^\top L_{ul} X_l + X_l^\top L_l X_l \end{aligned}$$

C.3.2 Pseudo-inverse of PLP , definiteness conditions of $X^\top B$, SQP Direction Z

Several of the algorithms we describe necessitate computation of pseudoinverse-vector products of the perturbed Laplacian PLP —i.e. $(PLP)^\dagger u$. Here, we demonstrate that the computation of $(PLP)^\dagger u$ is computationally comparable to computing a standard laplacian pseudoinverse-vector product, $L^\dagger u$, for which there exist nearly linear-time solvers [43].

Proposition C.3 (Pseudo-inverse of $PL^{-1}P$). *Let $P = I - vv^\top$ for a unit vector v . Let $r_k = \{PL^{-1}P\}^\dagger u_{k-1}$. Then, the projection of r_k is*

$$Pr_k = \{PL^{-1}P\}^\dagger u_{k-1} = (I - \frac{\bar{v}^\top v}{v^\top \bar{v}})L^{-1}u_{k-1}, \quad \bar{v} = L^{-1}v$$

Proposition C.4 (Definiteness conditions of $X^\top B$). *Assume $C = I$. Note the first term of F satisfies the invariance $\text{tr}(X^\top PLPX) = \text{tr}(\tilde{X}^\top PLP\tilde{X})$, where $\tilde{X} = XQ$ for any orthogonal $Q \in \mathbb{R}^{2 \times 2}$. X is a local minimizer if $X^\top B \succcurlyeq 0$ and symmetric.*

Proof. Note that by assumption, X is feasible—i.e. $X^\top X = I$. Consider the substitution $X \rightarrow XQ$ for some orthogonal matrix Q . Since $C = I$, $F(XQ) = \langle XQ, LXQ \rangle - \langle Q, X^\top B \rangle$.

Fix X . Note that the first term satisfies the invariance $\langle X, LX \rangle = \langle XQ, LXQ \rangle$. For any orthogonal $Q \in \mathbb{R}^{k \times k}$. The optimal choice of Q is determined by the second term. A standard result from matrix analysis yields its minimizer [22]. Let $X^\top B = UDV^\top$ be the SVD of $X^\top B$. Then, $Q = U_B V_B^\top$ and $\langle XQ, B \rangle = \langle Q, X^\top B \rangle = \langle I, D \rangle = \text{tr}(D) \geq 0$. \square

Proposition C.5 (SQP Direction of the Lagrangian Eq. eq. (10)). *Assume Λ symmetric. Let P and $\Lambda C^{-1} = U \text{diag}([\lambda_1, \dots, \lambda_k])U^{-1}$ be the eigenvector decomposition of ΛC^{-1} . The solution to the newton direction Z of X via the linearization of the FOC is given by*

$$Z = OU^\top \tag{27}$$

where each column of O , $o_j = (PLP - \lambda_j P)^\dagger BC^{-1}u_j$.

Proof. Recall the FOC and its associated linearization with respect to descent directions of X, Λ ; (Z, Δ) :

$$\begin{aligned} (LZC - Z\Lambda) - X\Delta &= E := BC^{1/2} - (LXC - X\Lambda) \\ X^\top Z &= 0 \end{aligned}$$

Applying the projection $P^\perp = I - XX^\top$ eliminates the $X\Delta$ term:

$$PLZ - Z\Lambda C^{-1} = PLPZ - ZU \text{diag}([\lambda_1, \dots, \lambda_k])U^{-1} = PEC^{-1}$$

Equivalently,

$$PLPZU - ZU \text{diag}([\lambda_1, \dots, \lambda_k]) = PEC^{-1}U.$$

Let $O = ZU = [o_1, \dots, o_k]$ lie in the range of P . Then,

$$PLO_j - \lambda_j = PEC^{-1}u_j, \text{ so } o_j = (PLP - \lambda_j P)^\dagger EC^{-1}u_j.$$

\square

C.4 Convergence of the Projected Gradient Method (PGD)

We first introduce a projected gradient-based method. With appropriate step size $\alpha > 0$, PGD produces iterates X_t , $t = 1, 2, \dots$

$$X_{t+1} = [X_t - \alpha g_t]_+$$

Where g_t is given by the gradient of the objective of eq. (23)—i.e. $g_t = LX_t C - BC^{1/2}$ and $[X_t]_+$ is the projection onto the manifold

$$\mathcal{M} := \{X : X \in \text{St}(n, k), X^\top B \geq 0\}$$

We first describe the projection $X = [X_1]_+$ as a composition of two projections; i.e. $[X_1]_+ = [[X_1]_{St}]_{\mathcal{B}} \in \mathcal{M}$:

$$Z = [X_1]_{St} := \arg \min_Z \{\|X_1 - Z\|_F : Z \in St(m, r)\} \quad (28)$$

$$X = [Z]_{\mathcal{B}} := ZQ, \quad Q = \arg \min_Q \{\|Z - BQ^T\|_F : Q \in O_k\} \quad (29)$$

In other words, $Z \in St(n, r)$ and $Q \in O_k$ are chosen to minimize the sum

$$\|X_1 - Z\|_F^2 + \|Z - BQ^T\|_F^2 = \|X_1Q - ZQ\|_F^2 + \|ZQ - B\|_F^2$$

Take the SVD of X_1 , i.e. $X_1 = U_X D_X V_X^T$. Then, the solution to eq. (28) is given by $Z = U_X V_X^T$. Likewise, $X = ZQ$ for some orthogonal matrix Q chosen to maximize $\langle X, B \rangle = X^T B$.

Proposition C.6 (Projection onto \mathcal{B}). *Consider the solution to the following projection:*

$$[X_1]_+ = \arg \min_{X \in St(n, k)} \left\{ \min_Q \|X - X_1Q\|_F^2 : X^T B \geq 0, Q \in O_k \right\} \quad (30)$$

Suppose the singular values of X_1 and B are positive. Then, the minimizer X is uniquely determined by

$$X = [X_1]_+ = U_1 U_2 V_2^T$$

where U_1, V_1, V_2 are determined from the two SVDs,

$$U_1 \Sigma_1 V_1^T = X_1, \quad U_2 \Sigma_2 V_2^T = U_1^T B$$

Proof. The minimizer X in eq. (30) is the maximizer of $\max_X \langle X, X_1Q \rangle$. Note that

$$\langle X, X_1Q \rangle = \langle X, U_1 \Sigma_1 V_1^T Q \rangle = \langle U_1^T X Q^T V_1, \Sigma_1 \rangle \leq \text{tr}(\Sigma_1)$$

Note two observations: (1) that $U_1^T X Q^T V_1$ lies in O_k , and (2) that equality holds if and only if $U_1^T X Q^T V_1 = I_k$ for some $X Q^T V_1 \in St(n, k)$, i.e. $X Q^T V_1 = U_1$, and thus,

$$X = U_1 V_1^T Q.$$

Furthermore, the condition $X^T B$ is symmetric and positive definite implies a choice of Q that fulfills

$$X^T B = Q^T V_1 U_2 \Sigma_2 V_2^T, \quad \text{i.e., } V^T Q = V_2 U_2^T$$

Finally, note that since the singular values Σ_1, Σ_2 are distinct and positive, U_1 and V_1 are uniquely determined up to column-sign $Q_1 = \text{diag}(\pm 1, \dots, \pm 1)$. Likewise, U_2 and V_2 are uniquely determined up to $Q_2 = \text{diag}(\pm 1, \dots, \pm 1)$. Hence,

$$X = U_1 Q_1 Q_2^T U_2 Q_2 Q_2^T V_2^T = U_1 U_2 V_2^T$$

is unique. \square

Remark C.2. Consider the function $h(X) = [X]_{St}$ defined on $\mathbb{R}^{n \times k}$ and $X \in St(n, k)$. The differential $\mathbb{D}h$ at X is the linear map given by

$$\mathbb{D}h(X)[T] - \lim_{\alpha \rightarrow 0} \alpha^{-1} (h(X + \alpha T) - h(X)) = (I - X X^T)T + (-1/2)X(T^T X - X^T T)$$

for each $T \in \mathbb{R}^{n \times k}$. When $X \in \mathcal{M}$ and $T = -(LXC - BC^{1/2})$, then

$$\langle T, \mathbb{D}h(X)[T] \rangle = \|(I - X X^T)T\|_F^2.$$

Proposition C.7. Let $d_t = -(LX_t C - BC^{1/2})$. Let $\{X_t\}$ be a sequence generated by the gradient projection method

$$X_{t+1} = [x_t + \alpha_t d_t]_+$$

where α_t is chosen according the Armijo rule. Then, every limit point of $\{X_t\}$ is a stationary point.

Proof. The proof is motivated by the proof by contradiction of Prop. 1.2.1 in Bertsekas [9].

Let $\mathcal{G}(X) = (I - X^\top X)(AXC - BC^{1/2})$ be the projected gradient of the objective of 23, F at X . We define α given by the Armijo rule—i.e. let $s > 0$, $\sigma \in (0, 1)$ and $\beta \in (0, 1)$. $\alpha_t = \beta^{m_t} s$, where m_t is the first nonnegative integer m for which

$$F(X_t) - F([X_t + \beta^m s d_t]_+) \geq -\sigma \beta^m s \langle \mathcal{G}(X_t), d_t \rangle$$

Suppose $\hat{X} \in \mathcal{M}$ is a limit point of $\{X_t\}$ with $\|\mathcal{G}(\hat{X})\| > 0$. By definition, $\{F(X_t)\}$ is monotonically nonincreasing to $F(\hat{X})$, i.e. $F(X_t) - f(X_{t-1}) \rightarrow 0$. By definition, since the α_t , the step sizes are generated via the Armijo rule, α_t satisfies

$$\begin{aligned} F(X_t) - F(x_{t+1}) &\geq F(X_t) - F([X_t + \alpha_t d_t]_+) \\ &\geq -\sigma \langle \mathcal{G}(X_t), d_t \rangle = \sigma \alpha_t \|\mathcal{G}(X_t)\|_F^2 \end{aligned} \quad (31)$$

Let $\{X_t\}_{\mathcal{T}}$ be a subsequence converging to $\hat{X} \in \mathcal{M}$. Since

$$\limsup_{t \rightarrow \infty} -\langle \mathcal{G}(X_t), d_t \rangle = \|\mathcal{G}(\hat{X})\|^2 > 0,$$

eq. (31) implies $\{\alpha_t\}_{\mathcal{T}} \rightarrow 0$. From Armijo's rule, for some $t' \geq 0$, the inequality

$$F(X_t) - F([X_t + \alpha_t \beta^{-1} d_t]_+) < -\sigma \alpha_t \beta^{-1} \langle \mathcal{G}(X_t), d_t \rangle \quad (32)$$

holds for all $t \geq t'$. By taking a subsequence $\{d_t\}_{\mathcal{T}'}$ of $\{d_t\}_{\mathcal{T}}$ such that $\{d_t\}_{\mathcal{T}'} \rightarrow d'$ and $X_t \rightarrow X'$, applying the mean value theorem to the left hand side of eq. (32), we have that

$$\begin{aligned} & -\langle L([X_t + \alpha'_t d_t]_+ C) - B, \mathbb{D}([X_t + \alpha'_t d_t]_+) [d_t] \rangle \\ &= (\alpha_t \beta^{-1})^{-1} (F(X_t)) - F([X_t + \alpha_t \beta^{-1} d_t]_+) \\ &< -\sigma \langle \mathcal{G}(X_t), d_t \rangle \end{aligned}$$

for some $\alpha'_t \in [0, \alpha_t \beta^{-1}]$. Taking the limit as $k \rightarrow \infty$, we have that $\alpha'_t \rightarrow 0$ and $\mathbb{D}([X_t + \alpha'_t d_t]_+) [d_t] \rightarrow \mathcal{G}(X')$, which implies

$$-\langle \mathcal{G}(X'), d' \rangle \leq -\sigma \langle \mathcal{G}(X'), d' \rangle, \text{ i.e. } -(1 - \sigma) \langle \mathcal{G}(X'), d' \rangle \leq 0$$

Since $\sigma < 1$, it follows that

$$-\langle \mathcal{G}(X'), d' \rangle = \|\mathcal{G}(X')\|_F^2 \leq 0$$

which contradicts the non-stationarity of X' . Hence, the limit point \hat{X} is a stationary point. \square

C.5 Convergence of SSM

The proof follows from the associated result for the Projected Gradient Method, Prop. C.7—i.e. applying the Projected Gradient Method with step sizes chosen according to the Armijo rule ensures that any limit point X_* is a stationary point, when $d_t = -(LX_t C - BC^{1/2}) \in S_t$. Let V_t be an isometry, consisting of vectors in S_t computed via a QR-factorization. Let $L_t := V_t^\top L V_t$ and $B_t = V_t^\top B$. Then, $F(\tilde{X}; L_t, B_t)$ be the corresponding objective in S_t . SSM computes $X_{t+1} = V_t \tilde{X}$, where

$$\tilde{X} := \arg \min_{\tilde{X}} F(\tilde{X}; L_t, B_t)$$

Note that the sequence $\{X_1, \dots, X_t, \dots\}$, with $X_{t+1} \in V_t$ monotonically reduces F with respect to t :

$$\begin{aligned} F(\tilde{X}; L_t, B_t) &= \frac{1}{2} \langle X_{t+1}, LX_{t+1} C - 2BC^{1/2} \rangle \\ &\leq \min_{\tilde{X}} \left\{ \frac{1}{2} \langle V_t \tilde{X}, L V_t \tilde{X} C - 2BC^{1/2} \rangle = \frac{1}{2} \langle \tilde{X}, L_t \tilde{X} C - 2B_t C^{1/2} \rangle = F(\tilde{X}; L_t, B_t C^{1/2}) \right\} \\ &\leq \frac{1}{2} \langle X_t, L X_t C - 2BC^{1/2} \rangle = F(X_t; L, B) \end{aligned}$$

For each t , since the columns of X_t and $LX_t C - BC^{1/2}$ lie in S_t , the iterations of the gradient projection method with Armijo rule lie in S_t , and the sequence with decreasing objective reaches a stationary point \tilde{X} , it is ensured that the first order condition

$$A X_* C - B C^{1/2} = X_* \Lambda_*$$

holds for some matrix $\Lambda_* \in \mathbb{R}^{k \times k}$, given by

$$\Lambda_* = X_*^\top (LX_*C - BC^{1/2}) = \lim_t X_t^\top (LX_kC - BC^{1/2})$$

In the case $C = I$, the following states that the inclusion of $[v_1, \dots, v_k]$ in S_t improves the quality of the stationary point X_* , characterized by the eigenvalues of Λ .

Proposition C.8 (Convergence of SSM). *Assume $C = I$. Let $X_* := [x_1, \dots, x_k]$ be a stationary point generated from SSM. Then,*

$$LX_* - X_*\Lambda_* = B.$$

Let $\lambda_1, \dots, \lambda_k$ be the eigenvalues of Λ_* and let the eigenvalues of L be $d_1 \leq d_2 \leq \dots \leq d_n$. Then, $\max\{\lambda_1, \dots, \lambda_k\} \leq d_k$.

Proof. Let $X_t = [x_{1,t}, \dots, x_{k,t}]$ be a global minimizer in V_{t-1} . let $Y_t := [y_{1,t}, \dots, y_{k,t}] = V_{t-1}^\top [x_{1,t}, \dots, x_{k,t}]$. Then,

$$L_{t-1}Y_t - B_{t-1} = Y_t\Lambda_t$$

holds for some Λ_k with eigenvalues $[\lambda_{1,t}, \dots, \lambda_{k,t}]$. In addition, since $Y_t B_{t-1} = X_t B$, then $X_t B$ is positive semidefinite and symmetric. As $t \rightarrow \infty$, $X_*^\top B$ is also positive semidefinite and symmetric. Additionally, let

$$P_j^{\perp,(t)} = I - \sum_{i \in \mathcal{R}-j} y_{i,t} y_{i,t}^\top.$$

The second order condition implies

$$P_j^{\perp,(t)} L P_j^{\perp,(t)} - \lambda_{j,t} P_j^{\perp,(t)} \succeq 0.$$

Consider the optimality of $x_{1,t}$. Let $\phi_{1,t}$ by a unit vector orthogonal to $[x_{2,t}, \dots, x_{k,t}]$ in $\text{span}\{v_1, \dots, v_k\}$. Then $P_j^{\perp,(t)} V_{t-1}^\top \phi_{1,t} = V_{t-1}^\top \phi_{1,t}$ holds and the second order condition yields

$$\begin{aligned} 0 &\leq \langle V_{t-1}^\top \phi_{1,t}, (P_j^{\perp,(t)} L P_j^{\perp,(t)} - \lambda_{j,t} P_j^{\perp,(t)}) V_{t-1}^\top \phi_{1,t} \rangle \\ &= \langle \phi_{1,t}, (L - \lambda_{1,t} I) \phi_{1,t} \rangle \\ &\leq (\min_i d_i - \lambda_{1,t}) \|\phi_{1,t}\|^2, \end{aligned}$$

Which implies $\lambda_{1,t} \leq \min_i d_i$. As $t \rightarrow \infty$, a subsequence of $\{x_{1,t}, \dots, x_{k,t} : t\}$ converges to $[x_1, \dots, x_k] \in \mathcal{M}$ and $\lambda_{1,t}$ converges to λ_1 . Hence, $\lambda_1 \leq \min_i d_i$. Likewise, $\lambda_j \leq \min_i d_i$ by the optimality of $x_{j,t}$ for $j = 2, \dots, k$. \square

The following is the result of Proposition C.8.

Theorem 1 (Global convergence of SSM). *A limit X_* of $\{X_1, X_2, \dots, X_t, \dots\}$ generated by SSM is a local minimizer of eq. (8).*

Note on convergence to globally optimal solutions

We briefly and informally discuss the necessary conditions for *global optimality* of eq. (9), under the assumption that $C = I$. For simplicity, take $k = 2$. And denote λ_1, λ_2 the eigenvalues of Λ . We can prove that for any local minimizer X , if the associated eigenvalues λ_1, λ_2 are both less than d_1 , the smallest nonzero eigenvalue of L , that X is a global minimizer. As we have shown, with proper initialization, our method recovers a local minimizer X such that λ_1, λ_2 are both less than d_2 . There are several potential avenues to prove that any local minimizer is also a global minimizer. For example we could impose an eigenvector-preserving transformation to L or restrict our analysis to graphs such that $\lambda_i = \lambda_k$ where $\lambda_i \geq 0$.

An alternative method is to ensure a non-degenerate condition on B as in canonical trust-region methods. Briefly, let v_1, \dots, v_k be the eigenvectors of L corresponding to k smallest nonzero eigenvalues $d_1 \leq \dots \leq d_k$. At a high level, we need to ensure that the columns of B are not nearly orthogonal to v_1, \dots, v_r .

Proposition C.9. *Let $V = [v_1, v_2] \in \mathbb{R}^{n \times 2}$ be the eigenvectors of L corresponding to the smallest two nonzero eigenvalues $d_1 \leq d_2$. Let X be a local solution satisfying the first order condition*

$$AX = X\Lambda + B$$

and second order condition $\lambda_1, \lambda_2 \leq d_2$. Let s_1 be the smallest singular value of $V^\top B$. Suppose

$$s_1 > d_2 - d_1$$

Then, the eigenvalues λ_1, λ_2 of the Lagrangian multipliers Λ are less than d_1 and X is a global minimizer.

Proof. Recall that the second order condition is

$$\lambda_j \leq d_2 \text{ for } j = 1, 2.$$

Consider the first order condition $LX = X\Lambda + B$. Taking an inner product with v_2 and v_1 yields

$$\begin{aligned} d_2 v_2^\top X &= v_2^\top LX = (v_2^\top X)\Lambda + v_2^\top B, \\ d_1 v_1^\top X &= v_1^\top LX = (v_1^\top X)\Lambda + v_1^\top B. \end{aligned}$$

Let u_1 and u_2 be eigenvectors of Λ associated with eigenvalues λ_1, λ_2 . For $j = 1, 2$, taking the product with u_j on the r.h.s yields

$$(d_2 - \lambda_j)v_2^\top X u_j = v_2^\top B u_j, \quad (d_1 - \lambda_j)v_1^\top X u_j = v_1^\top B u_j$$

Since $\|V\| = 1 = \|X\|$, then $\|V^\top X u_j\| \leq \|X u_j\| \leq 1$. Thus,

$$|d_2 - d_1| < s_1 \leq \|V^\top B u_j\| \leq \min(|d_2 - \lambda_j|, |d_1 - \lambda_j|) \|V^\top X u_j\| \leq \min(|d_2 - \lambda_j|, |d_1 - \lambda_j|)$$

which implies $\lambda_j < d_1$.

D Limitations and Societal Impact

Here, we list several limitations and briefly touch upon the broader societal impact of our method.

- **Optimization variance:** Our methods exhibit slightly larger variance predictions compared to Poisson learning. However, when our method is augmented with the KL refinement scheme, we see a significant decrease in the variance of predictions. In future work we intend to explore (1.) why SSM introduces variance in the solution and (2.) why cut-based refinement seems to remedy this issue.
- **Underlying graph structure:** Much of this work relies on the structure of the underlying graph. In this work, we did not explore variations on the graph structure and setting the graph weights, instead opting for a relatively simple approach via neural networks to generate features for each node.

We have introduced a new method for graph learning that improves on the state of the art across multiple label-rate regimes. The development of such methods has positive and negative ramifications for civil liberties and human rights. While the positive ramifications are relatively clear- models which require less data are cheaper to train and are generally “lower-impact”—the negative consequences are not immediately obvious. The above question is explored in greater detail in the content of semi-supervised graph learning in Fairness in graph-based semi-supervised learning, Zhang et al. [50]. The principal claim made by Zhang et al. [50] is that when quantities of unlabeled data are provided, label propagation may be modified to improve fairness. Interestingly, there seems to be an intimate relationship between methods designed to promote fairness and the cut-based MBO scheme proposed in Calder [12].